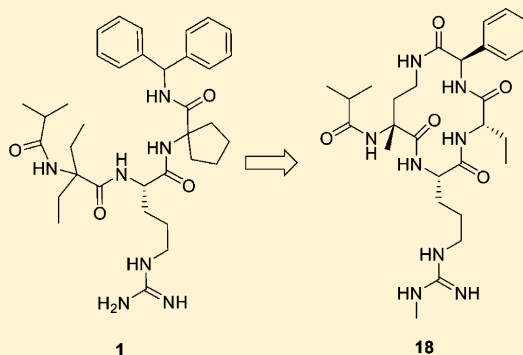


Discovery of a Highly Potent, Cell-Permeable Macrocyclic Peptidomimetic (MM-589) Targeting the WD Repeat Domain 5 Protein (WDR5)–Mixed Lineage Leukemia (MLL) Protein–Protein Interaction

Hacer Karatas,^{†,‡,§,Δ} Yangbing Li,^{†,‡,§,Δ} Liu Liu,^{‡,§,Δ} Jiao Ji,^{‡,§,Δ} Shirley Lee,^{||,Δ} Yong Chen,^{⊥,#} Jiuling Yang,^{‡,§,○} Liyue Huang,^{‡,§} Denzil Bernard,[‡] Jing Xu,^{||} Elizabeth C. Townsend,^{||} Fang Cao,^{||} Xu Ran,^{†,‡,§} Xiaoqin Li,[▽] Bo Wen,[▽] Duxin Sun,^{#,▽} Jeanne A Stuckey,^{§,#,¶} Ming Lei,^{⊥,#} Yali Dou,^{§,||} and Shaomeng Wang^{*,†,‡,§,○,||}[†]Department of Medicinal Chemistry, [‡]Department of Internal Medicine, [§]Comprehensive Cancer Center, ^{||}Department of Pathology, [⊥]Howard Hughes Medical Institute, [#]Department of Biological Chemistry, [▽]Department of Pharmaceutical Sciences, [○]Department of Pharmacology, and [¶]Life Sciences Institute, University of Michigan, Ann Arbor, Michigan 48109, United States

Supporting Information

ABSTRACT: We report herein the design, synthesis, and evaluation of macrocyclic peptidomimetics that bind to WD repeat domain 5 (WDR5) and block the WDR5–mixed lineage leukemia (MLL) protein–protein interaction. Compound **18** (MM-589) binds to WDR5 with an IC_{50} value of 0.90 nM (K_i value <1 nM) and inhibits the MLL H3K4 methyltransferase (HMT) activity with an IC_{50} value of 12.7 nM. Compound **18** potently and selectively inhibits cell growth in human leukemia cell lines harboring MLL translocations and is >40 times better than the previously reported compound MM-401. Cocrystal structures of **16** and **18** complexed with WDR5 provide structural basis for their high affinity binding to WDR5. Additionally, we have developed and optimized a new AlphaLISA-based MLL HMT functional assay to facilitate the functional evaluation of these designed compounds. Compound **18** represents the most potent inhibitor of the WDR5–MLL interaction reported to date, and further optimization of **18** may yield a new therapy for acute leukemia.



INTRODUCTION

Mixed lineage leukemia (MLL) protein, also known as MLL1 to distinguish it from other MLL family members (MLL2–MLL4), is a histone H3 lysine 4 (H3K4) methyltransferase. Although MLL has a role in normal hematopoiesis, it is frequently misregulated in a subset of human acute leukemias.^{1,2} Chromosomal translocations at 11q23 lead to more than 70 MLL fusion proteins, which result in aggressive leukemia with very poor prognosis and treatment outcome.^{1,3} MLL fusion occurs in nearly 70% of acute lymphoid leukemia (ALL) in infants and 5–10% of acute myeloid leukemia (AML) in adults.^{4–6}

Interestingly, MLL translocations invariably occur on only one MLL allele, and the MLL fusion proteins paradoxically display loss of the H3K4 methyltransferase activity. However, the remaining wild-type MLL allele, which retains the H3K4 methyltransferase activity, has been shown to be required for MLL-AF9-induced leukemogenesis and maintenance of MLL-AF9-transformed cells.^{7,8} Therefore, we, and others, have proposed that inhibition of the H3K4 methyltransferase activity of wild-type MLL protein may represent a new therapeutic

strategy for the treatment of aggressive leukemia harboring MLL fusion proteins.^{9–11}

Although MLL protein contains a catalytic SET domain for its H3K4 methyltransferase activity (HMT), the enzymatic activity is very low when MLL protein is present in isolation. However, the enzymatic activity of MLL is dramatically enhanced in a core complex consisting of MLL, WDR5 (WD repeat domain 5 protein), ASH2L (Absent, Small, or Homeotic-2-Like), and RbBP5 (Retinoblastoma Binding Protein 5).¹² Hence, targeting protein–protein interactions (PPIs) in the MLL core complex could be an effective strategy to inhibit the H3K4 HMT activity of MLL.

Among several PPIs within the MLL core complex, the WDR5–MLL interaction is particularly attractive for the design of small-molecule inhibitors to inhibit the MLL HMT activity. First, the WDR5–MLL interaction is essential for the formation of the MLL core complex and for the HMT activity of the MLL complex. Second, the interaction of MLL with

Received: December 9, 2016

WDR5 has been mapped to a 12-residue WIN (WDR5 interacting) motif (residues 3762–3773), which provided a good starting point for the design of small-molecule inhibitors.^{9,13} Third, the cocrystal structure of WDR5 protein in complex with the 12-residue MLL WIN peptide has shown that MLL binds to a well-defined pocket in WDR5, which appears to be suitable for the design of drug-like, small-molecule inhibitors.

Our group has reported the first-in-class inhibitors of WDR5–MLL interaction.^{10,11,14} In our strategy, we have pursued the design of peptidomimetics to block the WDR5–MLL interaction.^{11,14} Recently, several nonpeptide, small molecule inhibitors were identified to disrupt WDR5–MLL interaction by high throughput screening on compound libraries and following optimization based on the cocrystal structures of the inhibitors with WDR5 protein.^{15–19} For example, OICR-9429¹⁶ (Figure 1) was discovered as a fairly

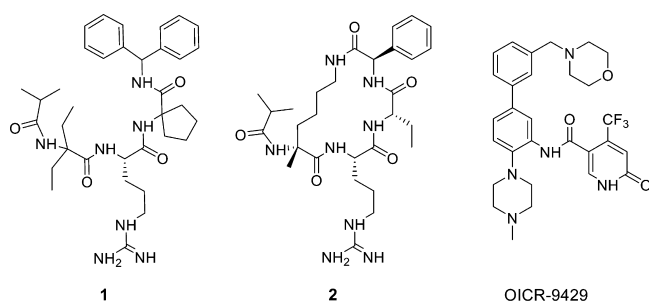


Figure 1. Chemical structures of three previously reported WDR5–MLL interaction inhibitors including a linear peptidomimetic, a cyclic peptidomimetic, and a nonpeptide inhibitor.

potent inhibitor of WDR5–MLL interaction and was used to explore the mechanism of p30-dependent transformation,

leading to the discovery that WDR5 is a therapeutic target in CEBPA mutant AML.²⁰

Previously, we determined that a 3-residue peptide (Ac-ARA-NH₂) binds to WDR5 with a K_i value of 120 nM, essentially the same as the 12-residue WIN peptide ($K_i = 160$ nM to WDR5 in the same assay).¹⁰ Further extensive modifications of the Ac-ARA-NH₂ peptide using both natural and unnatural amino acids have yielded a number of linear peptidomimetics with very high affinities to WDR5 with 1 (MM-101) being one of the best compounds (Figure 1).¹¹ Because these compounds mimic MLL WIN peptide for binding to WDR5, we also refer to them as MLL mimetics (MM).

Compound 1 binds to WDR5 with K_i value of <1 nM and potently and dose-dependently inhibits the MLL HMT activity in a fully reconstituted *in vitro* H3K4 methyltransferase assay.¹¹ However, linear peptidomimetic 1 has two major shortcomings: it has very modest cellular potency and poor metabolic stability in human microsomes. To improve cellular potency and microsomal stability, we have performed structure-based design, synthesis, and evaluation of conformationally constrained, macrocyclic peptidomimetics based upon the linear peptidomimetic 1. In the previous study,¹⁴ we have disclosed the design of one such cyclic peptidomimetic (compound 2 in Figure 1) and its extensive characterization for activity, specificity, and mechanism of action. In present study, we describe further design, synthesis, and biochemical and biological testing of a series of macrocyclic peptidomimetics. The present study has yielded a number of cyclic peptidomimetics that bind to WDR5 with very high affinities ($K_i \ll 1$ nM). In particular, we have identified a new cyclic peptidomimetic, 18, which is >40-times more potent than the reported cyclic peptidomimetic 2 in inhibition of cell growth in human leukemia cells harboring MLL translocations. Determination of the cocrystal structure of compound 18 in complex

Table 1. Chemical Structures, Binding Affinities to WDR5 and MLL HMT Inhibition Activities of Compound 2 and Its Analogues

Table 1 provides a summary of the chemical structures and activities of compounds 1 through 8. The structures show the positions of substituents R1, R2, R3, and R4 on the peptidomimetic backbone. Compound 8 is a cyclic peptidomimetic with a guanidine group.

compd	R ₁	R ₂	R ₃	R ₄	binding affinity to WDR5		inhibition of MLL HMT activity
					IC ₅₀ ± SD (nM)	K_i ± SD (nM)	IC ₅₀ ± SD (nM)
1	<i>a</i>	<i>a</i>	<i>a</i>	<i>a</i>	2.9 ± 1.4	<1	578 ± 190
2	-H	-H	-H	-H	0.9 ± 0.2	<1	373 ± 44
3	-H	-CH ₃	-H	-H	1.6 ± 0.3	<1	190 ± 33
4	-F	-CH ₃	-H	-H	1.6 ± 1.0	<1	138 ± 39
5	-Cl	-CH ₃	-H	-H	1.5 ± 0.9	<1	124 ± 28
6	-H	-H	-CH ₃	-H	1.1 ± 0.3	<1	452 ± 55
7	-H	-H	-CH ₃	-CH ₃	2.4 ± 0.7	<1	1259 ± 236
8	<i>a</i>	<i>a</i>	<i>a</i>	<i>a</i>	>10 000	>10 000	>10 000

^aNot applicable.

with WDR5 provides further structural insights for its high binding affinity to WDR5.

RESULTS AND DISCUSSION

Modification of Cyclic Peptidomimetic 2. Based upon the cocrystal structure of **2** in complex with WDR5, we designed and synthesized a series of new compounds to further determine the structure–activity relationships for this class of macrocyclic peptidomimetics. The results are summarized in Table 1.

The cocrystal structure of **2** in complex with WDR5 showed that the amino group connecting to the alkyl linker in **2** is exposed to solvent (Figure 2A).¹⁴ Computational modeling

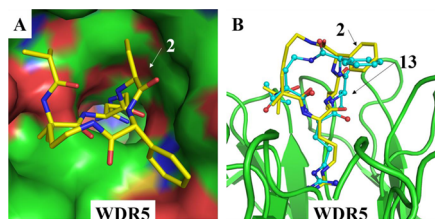


Figure 2. (A) Cyclic peptidomimetic **2** in complex with WDR5 [PDB ID 4GM9]. Compound **2** is shown in stick, and WDR5 is shown with surface model. (B) Superposition of the docked model of **13** (cyan) onto the cocrystal structure of compound **2** complexed with WDR5. Carbon atoms are shown in yellow for compound **2** or cyan for compound **13**, oxygen atoms are shown in red and nitrogen atoms are shown in blue.

indicated that methylation of this amino group would not distort the bound conformation. Since methylation of the amino group reduces the polar surface, it may improve cellular permeability and hence cellular activity. Accordingly, we have designed and synthesized compound **3**. Our previous study showed that *p*-F or *p*-Cl substitution on the phenyl group in linear peptidomimetics can enhance their cellular potency,¹¹ and compounds **4** and **5** with *p*-F or *p*-Cl substitution, respectively, on the phenyl group of **3** were therefore synthesized. The positively charged guanidine group in the arginine side chain was shown to be critical for binding of linear peptidomimetics to WDR5.¹¹ However, modeling studies suggested that guanidine group can tolerate both monomethylation and dimethylation maintaining strong interactions with WDR5. We, therefore, synthesized compounds **6** and **7** with monomethylation and symmetric dimethylation, respectively, on compound **2**.

Binding Affinities of Cyclic Peptidomimetics to WDR5.

We evaluated the binding affinities of these cyclic peptidomimetics to WDR5 using an optimized, FP-based competitive binding assay.¹⁰ The binding data showed that cyclic peptidomimetics **3**–**7** bind to WDR5 with IC₅₀ values of 1.1–2.4 nM with estimated K_i values of <1 nM (Table 1). Of note, because the affinities of these cyclic peptidomimetics exceed the lower assay limit of the FP-based competitive binding assay, their exact K_i values cannot be accurately determined. Nevertheless, the binding data showed that all these cyclic peptidomimetics have very high binding affinities to WDR5. In comparison, compound **8**, the enantiomer of **2**, has no appreciable binding to WDR5 at concentrations as high as 10 μM, indicating that the binding of compound **2** to WDR5 is stereospecific.

Development and Optimization of a New AlphaLISA based MLL HMT Functional Assay and Inhibition of the MLL HMT Activity by Cyclic Peptidomimetics. Because the WDR5–MLL interaction is required for the MLL complex to achieve robust H3K4 HMT activity, compounds that target this interaction are predicted to effectively inhibit the MLL H3K4 HMT activity. Since our previous MLL HMT functional assay utilizes radioactive ³H labeled S-adenosyl methionine (SAM), involves multiple wash and transfer steps and is, therefore, quite time-consuming,¹¹ we have developed and optimized a new, amplified luminescent proximity homogeneous assay (AlphaLISA) to evaluate the MLL HMT inhibitory activities of the newly designed cyclic peptidomimetics. The assay flow is shown in Figure 3A. In this assay, recombinant nucleosomes were initially treated with the MLL complex for methylation in the presence of S-adenosyl methionine (SAM) as cofactor before the reaction was stopped with high salt buffer. Then, anti-H3K4Me1/2 antibody, which is covalently linked to acceptor beads, and biotinylated anti-H3 (C-terminus) antibody were added. Lastly, streptavidin labeled donor beads were added, and the assay plate was imaged with a microplate reader using excitation wavelength of 680 nm and emission wavelength of 615 nm.

Different from widely used homogeneous time resolved fluorescence (HTRF) assays, in which energy transfer can only take place between donor–acceptor fluorophores located within approximate 10 nm, short-lived singlet oxygen (¹O₂) generated from AlphaLISA donor beads can reach the acceptor beads as far as 200 nm away. This extra-long effective range significantly enhances the versatility of Alpha assays, in which multiple labeled antibodies can be utilized. Such feature is also particularly useful for HMT functional assays involving large-size components, such as nucleosomes as substrates, which are 11 nm in size (e.g., mononucleosomes) or much larger (e.g., oligonucleosomes). Histone methylation assays that use nucleosomes as substrates more closely mimic the MLL HMT reaction in cells, compared with those that utilize histone peptide or proteins as substrates. Therefore, a functional AlphaLISA MLL HMT assay using nucleosomes as substrates would be highly valuable to evaluate these WDR5 inhibitors.

Although no robust MLL HMT AlphaLISA assay has been reported yet, the acceptor bead conjugated with antibodies that can recognize methylated H3K4 is commercially available and was used here to develop the MLL HMT AlphaLISA assay (Figure 3A). As indicated by the manufacturer and confirmed in our own experiments, this antibody can only recognize mono- and dimethylated H3K4. Therefore, we optimized assay conditions, described below, and paid particular attention to minimize trimethylation of nucleosomes, which would greatly compromise the interactions of acceptor beads with mono- and dimethylated nucleosomes and thereby significantly reduce fluorescence intensity detected in the assay yielding a low dynamic range.

We investigated the influence of reaction time and concentration of the MLL complex on fluorescence intensity using two different SAM concentrations (Figure 3B,C). At low SAM concentration (300 nM), AlphaLISA fluorescence signals increased with longer reaction time when MLL complex concentration was 1–5 nM, were steady with 10 nM MLL complex, but decreased as early as 30 min with 20 nM of the MLL complex. Furthermore, when SAM concentration was 10-fold higher (3 μM) with which reaction was even faster, only a

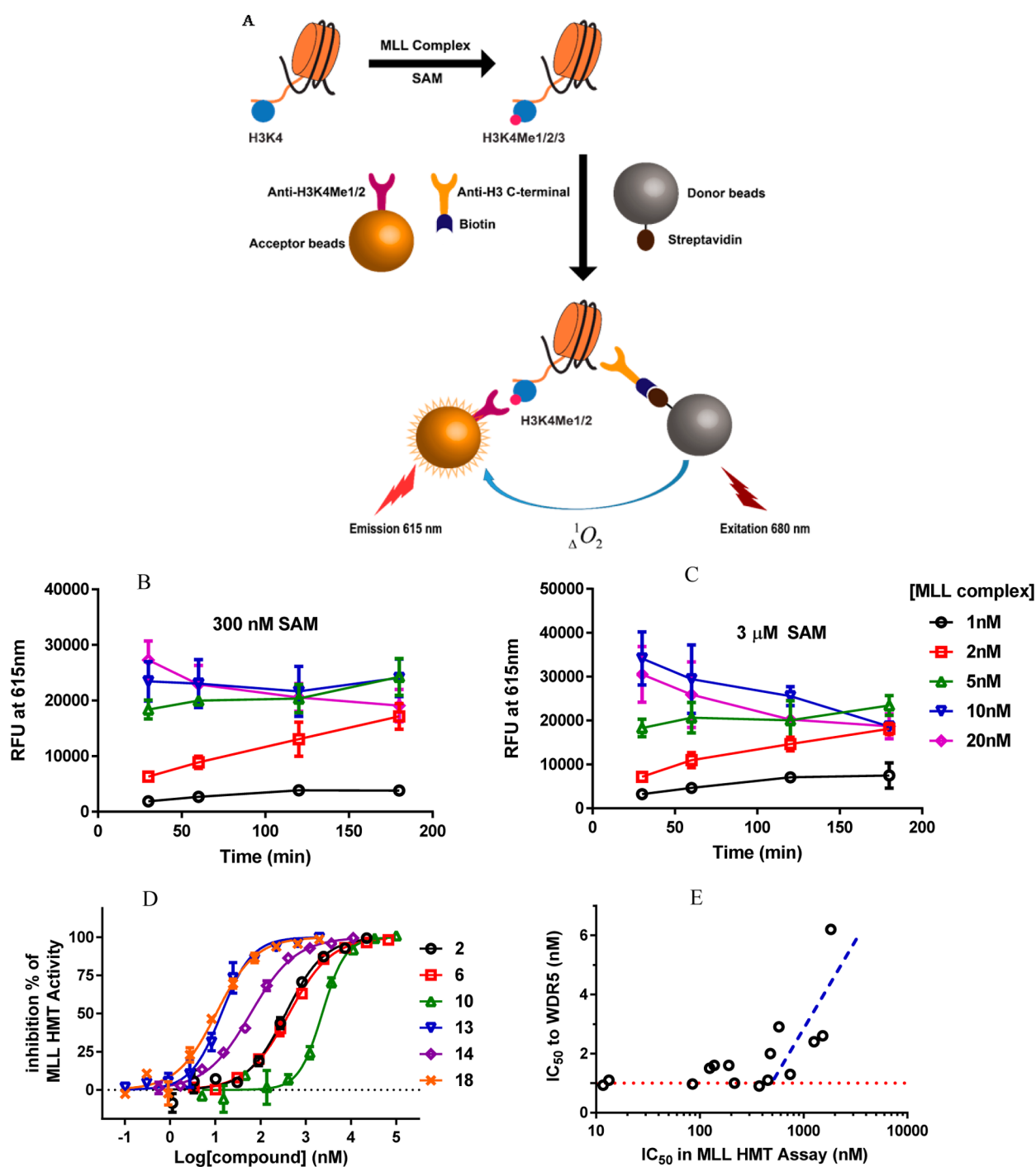


Figure 3. Development and optimization of a homogeneous AlphaLISA MLL functional assay. (A) Illustration of the homogeneous AlphaLISA MLL HMT functional assay. (B, C) Enzymatic activity of MLL complex, represented by the fluorescence intensity in relative fluorescence units (RFU) from acceptor beads detected at 615 nm at different concentrations and different reaction time points with a low (300 nM, B) or a high (3 μ M, C) SAM concentration. (D) Representative inhibitory curves of selected WDR5 inhibitors. (E) Comparison of potencies of compounds determined from the competitive WDR5 binding assay and the AlphaLISA MLL functional assay.

slight signal increase was observed when using 5 nM of the MLL complex and significant signal decrease started at 30 min with both 10 and 20 nM of the MLL complex. Consistent with the expectation, AlphaLISA signal decrease was observed with higher MLL complex concentrations, longer reaction time, and even more severely with higher SAM concentrations, which is most likely attributed to generation of more trimethylated nucleosomes.

Representative inhibitory curves of selected WDR5 inhibitors using the optimized AlphaLISA MLL HMT functional assay are shown in Figure 3D. This new functional assay was able to discriminate compounds with very high affinities to WDR5 as determined in the FP-based competitive binding assay. We thus compared the IC_{50} values obtained from the FP-based competitive binding assay with those obtained from the AlphaLISA functional assay for all the compounds included in the present study (Figure 3E). The data showed that there is

a linear correlation between the IC_{50} values obtained from WDR5 competitive binding assay (y -axis) and MLL HMT functional assay (x -axis) as shown with blue dashed line. However, compounds with IC_{50} values of 1–2 nM in the WDR5 competitive binding assay deviate from this linear correlation and have IC_{50} values ranging between 10 and 500 nM in the functional assay. These data indicate that this new MLL HMT functional assay can nicely discriminate highly potent WDR5 inhibitors, which is not possible with the FP-based competitive binding assay. IC_{50} values obtained for compounds 1–8 in this MLL functional assay are summarized in Table 1.

Functional data showed that linear peptidomimetic 1 effectively inhibits the MLL HMT activity with an IC_{50} value of 578 nM, and cyclic peptidomimetic 2 has an IC_{50} value of 373 nM. New compounds 3–5 achieve IC_{50} values of 124–190 nM in the HMT functional assay and are thus 2–3 times more potent than compound 2. Compound 6 with a monomethylated guanidine group has an IC_{50} value of 452 nM, which is slightly less potent than 2, and compound 7 with a dimethylated guanidine group is 3-times less potent than 2. Consistent with its weak binding affinity to WDR5, the control compound 8 fails to inhibit the MLL HMT activity at the highest concentration (10 μ M) tested. It should be noted that potencies determined in the MLL HMT assay for all the compounds reported in the present study are based on their ability to inhibit mono- and dimethylation activities of the MLL complex.

Activity and Selectivity of Cyclic Peptidomimetics To Inhibit Cell Growth of Human Leukemia Cell Lines. We next evaluated representative cyclic peptidomimetics 2, 4, 6, 7, and 8 in three human acute leukemia cell lines for their activity and selectivity in inhibition of cell growth. The data are summarized in Table 2. In the MV4-11 cell line harboring

Table 2. Inhibition of Cell Growth (IC_{50} , μ M) with Representative Cyclic Peptidomimetics

compd	MOLM-13	MV4-11	HL-60
2	18.4 \pm 6.6	9.8 \pm 8.0	>100
4	16.2 \pm 6.1	5.2 \pm 1.1	60.0 \pm 19.7
6	3.6 \pm 0.8	4.3 \pm 1.5	>100
7	31.5 \pm 9.8	15.2 \pm 2.9	84.8 \pm 13.2
8	>100	>100	>100

MLL-AF4 fusion protein and the MOLM-13 cell line harboring MLL-AF9 fusion protein, compound 2 has IC_{50} values of 9.8 and 18.4 μ M, respectively, similar to those values reported in the previous study.¹⁴ Compound 4 has comparable potencies as compound 2 in inhibition of cell growth in both the MV4-11 and MOLM-13 cell lines. Compound 7 is slightly less potent than 2 in both the MV4-11 and MOLM-13 cell lines. However, compound 6 has IC_{50} values of 3.6 (MOLM-13) and 4.3 μ M (MV4-11) and is 2–5 times more potent than 2. Compound 8, which has no appreciable binding to WDR5 and does not inhibit the MLL HMT activity at 10 μ M, has IC_{50} > 100 μ M in both the MV4-11 and MOLM-13 cell lines in the same cell growth inhibition assay, suggesting that cellular activity for the cyclic peptidomimetics in these two leukemia cell lines is specific and on-target.

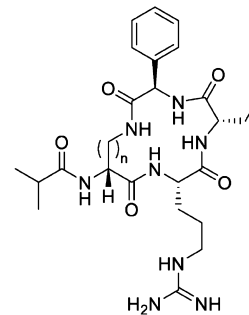
Next, we assessed specificity of cyclic peptidomimetics to inhibit cell growth in the HL-60 leukemia cell line lacking MLL translocation. Compounds 2, 6, and 8 have IC_{50} values of >100

μ M, and 4 and 7 have modest activity with IC_{50} values of 60.0 and 84.8 μ M, respectively. Hence, these cyclic peptidomimetics display cellular selectivity against the MV4-11 and MOLM-13 leukemia cell lines harboring MLL fusion proteins over the HL-60 cell line lacking MLL translocation.

Optimization of the Ring Size in These Cyclic Peptidomimetics. Since the length of the linker in the designed cyclic peptidomimetics plays a key role for their conformations, we have modeled compounds with different linker lengths. Interestingly, modeling suggested that cyclic peptidomimetics with a linker as short as 2-carbon appear to be able to adopt low-energy conformations that closely resemble the bound conformation of compound 2 (Figure 2B).

Since cyclic peptidomimetic 2 has a binding affinity exceeding the lower assay limit in the FP-based competitive binding assay, we sought to use a less potent cyclic peptidomimetic as the template to better understand the effect of the linker length on binding affinity to WDR5. For linear peptidomimetics, we have shown that the methyl group attached to the bridging carbon atom contributes significantly to their affinity to WDR5.¹¹ Indeed, removal of this methyl group in 2 yielded 12, which has a K_i value of 60.3 nM, >50-times less potent than 2. Compound 12 was thus used as the template for further investigation of the linker. The results are summarized in Table 3. Compound 9 with a one-carbon linker

Table 3. Chemical Structures, Binding Affinities to WDR5, and MLL HMT Inhibition Activities of Demethylated Analogues of Compound 2 with Different Linker Sizes



compd	n	binding affinity to WDR5		inhibition of MLL HMT activity
		$IC_{50} \pm SD$ (nM)	$K_i \pm SD$ (nM)	$IC_{50} \pm SD$ (μ M)
9	1	1190 \pm 160	242 \pm 33	>10
10	2	6.2 \pm 0.5	0.8 \pm 0.1	1.8 \pm 0.4
11	3	164 \pm 26	32.9 \pm 5.3	>10
12	4	298 \pm 58	60.3 \pm 11.9	>10

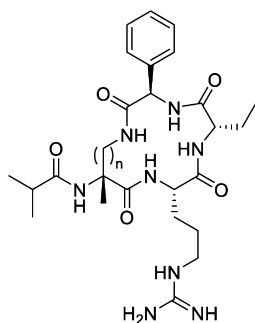
has K_i value of 242 nM to WDR5 and is thus 4-times less potent than 12 with a 4-carbon linker. However, compound 10 with a 2-carbon linker has K_i value of 0.8 nM to WDR5 and is >70-times more potent than 12. Compound 11 with a 3-carbon linker has K_i value of 32.9 nM to WDR5 and is 2-times more potent than 12. Hence, further investigation of the linker length showed that compound 10 with a 2-carbon linker achieves the highest binding affinity among this series of analogues.

We next tested these compounds (9–12) for their inhibitory activity in the newly established MLL HMT functional assay. Functional data showed that their potencies in inhibition of the MLL HMT activity correlate nicely with their binding affinities to WDR5. Accordingly, compound 10 has the best potency to

inhibit the MLL HMT activity ($IC_{50} = 1.8 \mu M$), while IC_{50} values of other compounds are higher than $10 \mu M$ (Table 3). These data further show that the newly established HMT functional assay can clearly distinguish the potency differences even among compounds with very high binding affinities to WDR5.

Design and Synthesis of Compound 2 Analogues with Different Ring Sizes. Based upon the promising data for compound 10, we synthesized and evaluated a series of analogues of compound 2 with different ring sizes with the results summarized in Table 4.

Table 4. Chemical Structures, Binding Affinities to WDR5, and MLL HMT Inhibition Activities of Compound 2 Analogues with Different Linker Length



compd	n	binding affinity to WDR5		inhibition of MLL HMT activity
		$IC_{50} \pm SD$ (nM)	$K_i \pm SD$ (nM)	$IC_{50} \pm SD$ (nM)
2	4	0.9 ± 0.2	<1	373 ± 44
13	2	1.08 ± 0.12	<1	12.6 ± 1.2
14	3	0.97 ± 0.13	<1	84.8 ± 23.8
15	5	2.6 ± 0.2	<1	1527 ± 218
16	6	1.0 ± 0.2	<1	216 ± 88
17	8	1.3 ± 0.2	<1	744 ± 79

Compounds 13, 14, 2, 15, 16, and 17 with linker lengths of 2, 3, 4, 5, 6, and 8 carbons, respectively, all bind to WDR5 with very high affinities ($IC_{50} = 0.9$ – 2.6 nM, $K_i < 1$ nM). Since the binding affinities of these compounds exceed the lower assay limit, the potential differences in their binding affinities to WDR5 cannot be discerned. However, the functional assay showed that while all of them can effectively inhibit MLL HMT activity, their potencies are not the same. Among these analogs, compound 13 has the best inhibitory activity with IC_{50} value of 12.6 nM, which is about 30-times more potent than 2. Compound 14 with a 3-carbon linker is the second most potent inhibitor of the MLL HMT activity with an IC_{50} value of 84.8 nM.

We next evaluated these compounds for their cell growth inhibitory activity in MOLM-13, MV4-11, and HL-60 cell lines (Table 5). Compound 10 displays modest cellular activities with IC_{50} values of $42.8 \mu M$ and $43.4 \mu M$ against MOLM-13 and MV4-11 cell lines, respectively, and compounds 11 and 12 have minimal activity at $100 \mu M$ in both cell lines. Compound 14 shows fairly potent cellular activity with IC_{50} values of 1.28 and $1.29 \mu M$ in the MOLM-13 and MV4-11 cell lines, respectively. Compound 13 (MM-581) is the most potent compound in this series and has IC_{50} values of 0.28 and $0.46 \mu M$, respectively, in inhibition of cell growth in the MOLM-13 and MV4-11 cell lines. Significantly, compounds 13 and 14

Table 5. Inhibition of Cell Growth (IC_{50} , μM) with Representative Cyclic Peptidomimetics

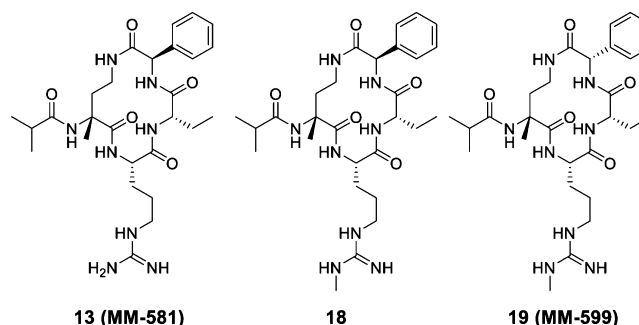
compd	MOLM-13	MV4-11	HL-60
2	18.4 ± 6.6	9.8 ± 8.0	>100
10	42.8	43.4	>100
11	>100	>100	>100
12	>100	>100	>100
13	0.28 ± 0.02	0.46 ± 0.02	17.4
14	1.28 ± 0.01	1.29	46.8
15	37.6 ± 12.1	15.1 ± 11.8	>100
16	5.6 ± 0.7	3.2 ± 0.4	29.7 ± 11.5
17	21.6 ± 4.8	7.5 ± 3.0	>100
18	0.21 ± 0.02	0.25 ± 0.01	8.56 ± 1.14
19	14.3 ± 0.9	35.0 ± 4.4	a

^aNot tested.

have much weaker activity in the HL-60 cell line lacking MLL translocation and display more than 30-fold cellular selectivity.

Further Modifications of Compound 13. Monomethylation of the guanidine group in compound 2, which yielded compound 6, improves cellular potency against MV4-11 and MOLM-13 cell lines (Table 2). We therefore monomethylated the guanidine group in compound 13, which yielded compound 18 (Table 6). Similar to compound 13, compound 18 binds to WDR5 with high affinity ($IC_{50} = 0.90$ nM, K_i value of <1 nM) and potently inhibits the MLL HMT activity ($IC_{50} = 12.7$ nM).

Table 6. Chemical Structures, Binding Affinities to WDR5, and MLL HMT Inhibition Activities of Compounds 13, 18, and 19



compd	binding affinity to WDR5		inhibition of MLL HMT activity
	$IC_{50} \pm SD$ (nM)	$K_i \pm SD$ (nM)	$IC_{50} \pm SD$ (nM)
13	1.08 ± 0.12	<1	12.6 ± 1.2
18	0.90 ± 0.20	<1	12.7 ± 1.5
19	2.0 ± 0.1	<1	477 ± 51

The specificity of compound 18 was tested against MLL and other SET1 family members (MLL2, MLL3, MLL4, SET1a and SET1b) using the previously published HMT assays.¹⁴ The data showed that while 18 effectively inhibits the MLL HMT activity ($IC_{50} = 12.7$ nM) in our new HMT assay, it has no or a minimal effect up to $100 \mu M$ in inhibition of the HMT activity of other SET1 family members (Figure S1).

Compound 18 was next evaluated for its activity and specificity to inhibit cell growth of acute leukemia cancer cell lines (Figure 4). Compound 18 achieves potent cell growth inhibitory activity in both the MV4-11 and MOLM-13 cell lines with IC_{50} values of 0.25 and $0.21 \mu M$, respectively. Compound 18 has much weaker activity in the inhibition of cell growth of

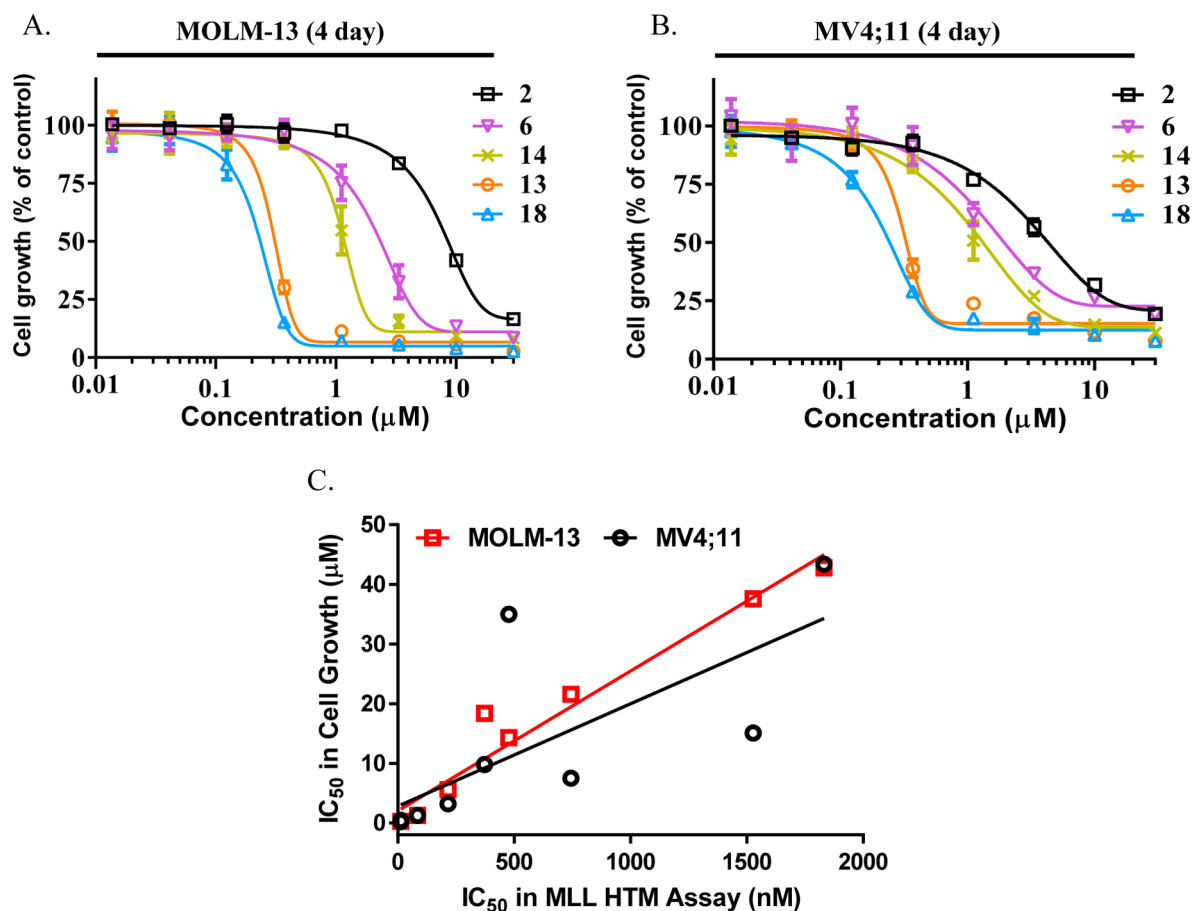


Figure 4. (A,B) Cell growth inhibition curves of representative cyclic peptidomimetics in MOLM-13 and MV4;11 human leukemia cell lines harboring MLL translocation. (C) Correlation between inhibition potencies of cell growth and MLL HMT activity of representative cyclic peptidomimetics.

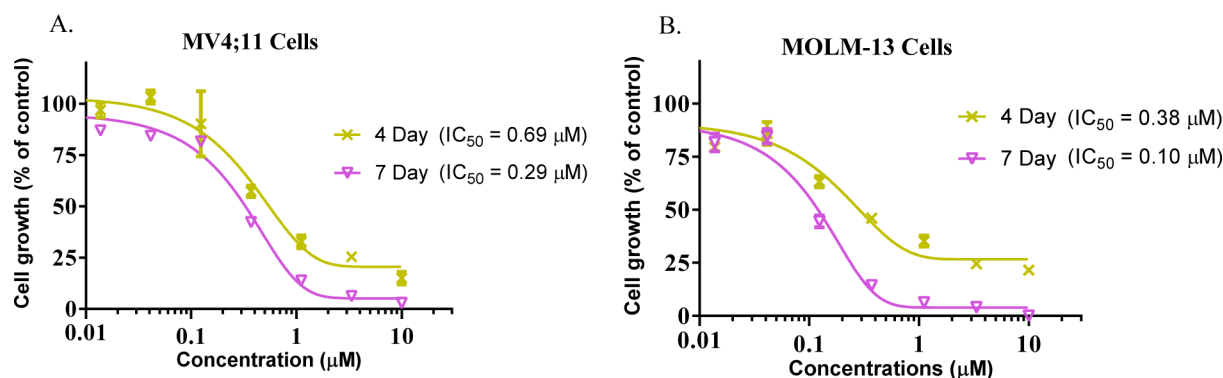


Figure 5. Cell growth inhibition of compound 18 upon 4-day or 7-day treatment time in MV4-11 and MOLM-13 acute leukemia cell lines.

the HL-60 cell line with an IC₅₀ value of 8.6 μM, hence displaying >30-fold selectivity for the MV4-11 and MOLM-13 cell lines harboring MLL translocations over the HL-60 cell line lacking MLL translocation.

To test the stereospecificity of 18, we synthesized compound 19 in which the chiral center in the phenylglycine residue is changed from D- to L-configuration (Table 6). Compound 19 still binds to WDR5 with a high affinity (IC₅₀ = 2.0 nM, K_i < 1 nM) but is 40-times less potent (IC₅₀ = 477 nM) than compound 18 (IC₅₀ = 12.7 nM) in inhibition of the MLL HMT activity (Table 6). Consistently, compound 19 has IC₅₀ values of 14.3 and 35.0 μM in inhibition of cell growth in

MOLM-13 and MV4-11 cell lines, respectively (Table 5), and is thus >50–100 times less potent than compound 18.

We next investigated whether there is a correlation between the potencies of cyclic peptidomimetics in inhibition of the MLL HMT activity and inhibition of cell growth of both MV4-11 and MOLM-13 cell lines. The analysis revealed that there is a fairly good correlation between the IC₅₀ values in inhibition of the MLL HMT activity (*x*-axis) and the IC₅₀ values of cell growth inhibition (*y*-axis) in both cell lines (Figure 4C).

Small molecule inhibitors targeting HMT activity, such as inhibitors of the EZH2 H3K27 activity²¹ and the DOT1L H3K79 activity,²² were shown to have very slow kinetics in

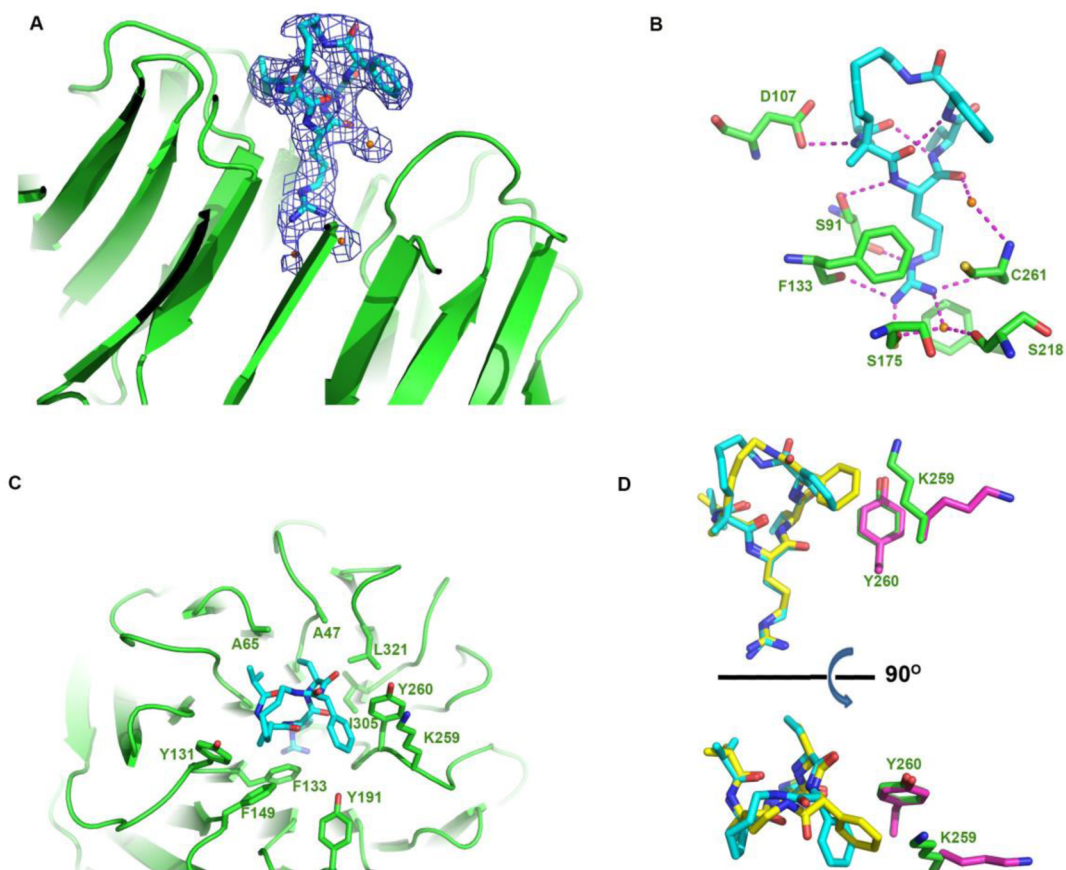


Figure 6. (A–C) Cocystal structure of compound **16** in complex with WDR5 (PDB ID 4GMB) and (D) in comparison with cocystal structure of **2** in complex with WDR5 (PDB ID 4GM9). Carbon atoms for compound **16** and compound **2** are shown in cyan and yellow, respectively. Nitrogen atoms are shown in blue and oxygen atoms are shown in red.

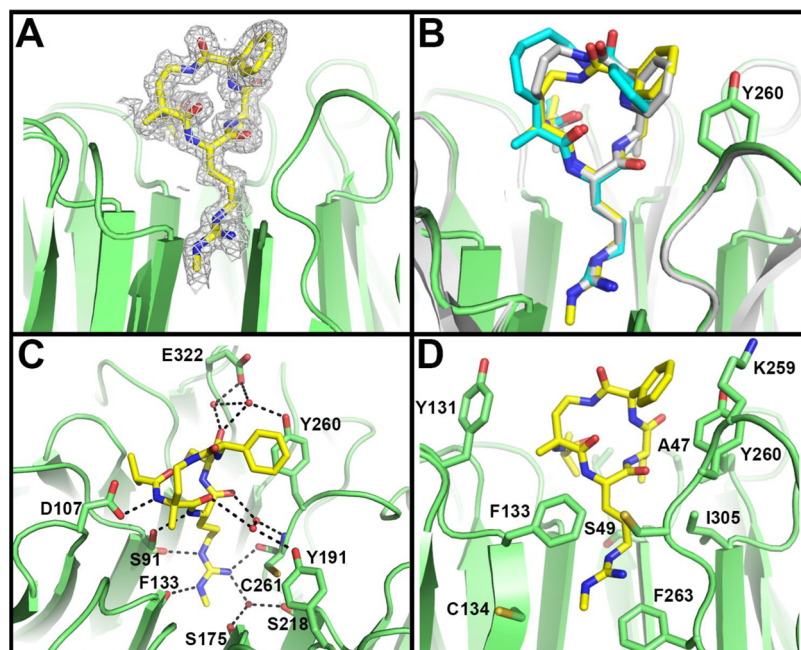


Figure 7. Cocystal structure of cyclic peptidomimetic **18** in complex with WDR5 (PDB ID 5VFC). (A) The unbiased difference electron density map for **18** contoured at 3σ is shown as a gray grid. (B) Structural alignment of WDR5–**18** with the cocystal structures of compounds **2** and **16** in complex with WDR5 (PDB ID 4GM9 and 4GMB, respectively). (C) The hydrogen bonding and (D) hydrophobic interactions of WDR5 and **18**. Dashed lines represent hydrogen bonds (C). Carbon atoms for compounds **18**, **16**, and **2** are shown in yellow, cyan and white, respectively. Nitrogen atoms are shown in blue and oxygen atoms are shown in red.

inhibition of cell growth. We therefore evaluated compound **18** for its inhibitory activity of cell growth in MV4-11 and MOLM-13 leukemia cell lines with either 4- or 7-day treatment. Although the IC_{50} values for **18** improved 2–3 times from 4-day treatment to 7-day treatment in both cell lines, the maximum inhibition has changed significantly, from partial inhibition to essentially complete inhibition (Figure 5). While approximately 75% maximum growth inhibition was achieved with **18** upon 4-day treatment in MV4-11 and MOLM-13 cell lines, > 95% maximum inhibition was achieved upon 7-day treatment in both cell lines. Of note, in this experiment, we seeded 100 000 cells in each well in 24-well plates, whereas the cell growth inhibition data obtained for compound **2** in Table 5 was obtained by seeding 10 000 cells in 96-well plates. Additionally, we have tested the stability of compound **18** in cell culture media up to 7 days and found that the compound is stable (Figure S3).

Determination of Cocrystal Structures of Compounds 16 and 18 in Complex with WDR5. We have previously reported a cocrystal structure of cyclic peptidomimetic **2** in complex with WDR5.¹⁴ To gain further structural insights into the high-affinity interactions of cyclic peptidomimetics with WDR5, we have obtained additional cocrystal structures. To date, we have successfully determined a cocrystal structure for compound **16** at a resolution of 2.8 Å (Figure 6, PDB code 4GMB) and a cocrystal structure for **18** in complex with WDR5 at a resolution of 1.64 Å (Figure 7, PDB code 5VFC).

The WDR5 component in the cocrystal structures of **16** and **18** adopts the same β -propeller configuration as the apo-WDR5 structure (PDB 2H14), with RMSDs (root-mean-square deviation) of 0.505 and 0.511 Å, respectively. The compounds were unambiguously placed into the central channel of WDR5 through the guidance of difference electron density maps. (Figures 6A and 7A). Compounds **16** and **18** bind to the central channel of WD40 propeller in WDR5 through the conserved interaction network as observed in WDR5/MLL and WDR5/2 cocrystal complex structures.¹⁴ In agreement with the previous WDR5/2 cocrystal structure, the arginine moiety in **16** and **18**, which is sandwiched between two phenyl rings from Phe133 and Phe263, engages in a complex array of hydrogen bonding with WDR5. The guanidinium moiety in **16** and **18** takes part in direct hydrogen bonds with Cys261, Phe133, and Ser91 and water-mediated hydrogen bonds with Ser218. The guanidinium moiety in **16** also forms a water-mediated hydrogen bond with Ser175. The N-terminal amide group of arginine in **16** and **18** forms a hydrogen bond with hydroxyl group of Ser91, and C-terminal carbonyl group of arginine engages in a water-mediated hydrogen bond with amide group of Cys261. Compounds **16** and **18** adopt a compact bound conformation mediated by 5 direct and 5 or 4 water mediated hydrogen bonds to WDR5 (Figure 6C).

The methyl group next to the guanidinium moiety in **18** gained hydrophobic interactions with Cys134 and Phe263 (Figure 7D). Complementary to these hydrogen bonds, the aliphatic carbon linker and side chains (methyl, isopropyl, ethyl, and phenyl groups) of both **16** and **18** make extensive hydrophobic packing against the hydrophobic surfaces surrounded by the side chains of Tyr131, Phe133, Tyr191, Tyr260, Leu321, Ile305, Ala47, and Ala65 from WDR5 (Figures 6C and Figure 7D). The different linker lengths in compounds **2**, **16**, and **18** lead to different orientations of the phenyl group in these compounds (Figures 6D and 7B). In compounds **2** and **18**, the phenyl group stacks nearly parallel to

the phenyl group of WDR5 Tyr260. In contrast, the phenyl group in **16** is oriented nearly perpendicular to the phenyl group of WDR5 Tyr260, comprising an incomplete aromatic cage. Interestingly, the side chain of WDR5 Lys259 is surrounded by an aromatic cage through cation– π stacking interactions (Figures 6D and 7D), which is reminiscent of the interaction mode observed in chromodomain recognition of methyl lysine.²³ Comparing with **2** and **16**, the smaller ring size of **18** forms a more compact structure, which facilitates the formation of several optimal intramolecular hydrogen bonds and reduces its conformational flexibility, allowing this compound to achieve a very high affinity to WDR5 and consequently high potency to inhibit the MLL HMT activity.

Overall, although cyclic peptidomimetics **2**, **16**, and **18** bind to WDR5 with similar binding modes, there are some differences observed in their structures and interactions with WDR5.

Microsomal Stability of Macrocyclic Peptidomimetics.

One significant shortcoming we observed for linear peptidomimetic **1** was that it has poor stability in human microsomes ($T_{1/2} = 4$ min) and moderate stability in mouse and rat microsomes ($T_{1/2} = 44$ min and $T_{1/2} = 34$ min, respectively). To determine whether cyclization has improved the microsomal stability, we evaluated a number of cyclic peptidomimetics for their stability in human, mouse, and rat microsomes, and the data are summarized in Table 7.

Table 7. Microsomal Stabilities ($T_{1/2}$, min) of Linear Peptidomimetic 1 and Selected Cyclic Peptidomimetics

compd	human	rat	mouse
1	4	34	44
2	>60	>60	>60
3	>60	>60	>60
4	>60	>60	>60
5	>60	>60	>60
13	>60	>60	>60
14	>60	>60	>60
16	21	>60	>60
18	>60	>60	>60

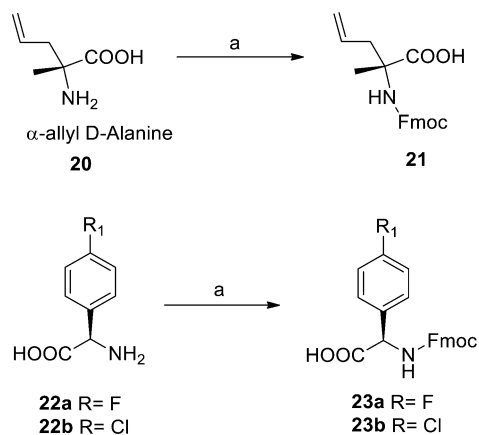
The microsomal stability data showed that **2**, **18**, and a number of other macrocyclic peptidomimetics all have excellent microsomal stability in human, mouse, and rat microsomes with half-life greater than 60 min, except for compound **16** with shorter half-life in human microsomes ($T_{1/2} = 21$ min).

Overall, the microsomal stability data show that **2**, **18**, and a number of other cyclic peptidomimetics have excellent microsomal stability in human, mouse, and rat microsomes, and their stability significantly improved over linear peptidomimetic **1**.

Chemical Synthesis. Synthesis of common intermediates for cyclic peptidomimetics is shown in Schemes 1 and 2. N-Termini of unnatural amino acids **20**, **22a**, and **22b** were protected with Fmoc group to give intermediates **21**, **23a**, and **23b**, respectively (Scheme 1).

Intermediates **25**, **27**, and **29** were prepared on the 2-chlorotrityl chloride resin (**24**) using solid phase peptide synthesis with Fmoc chemistry and cleaved from the resin to yield carboxylic acids **26**, **28**, and **30**, respectively (Scheme 2).

Synthesis of the designed cyclic peptidomimetics **2–7** and **15–17** is shown in Scheme 3. An alkeneamine (**31a–31e**) was first attached to an Fmoc-phenylglycine (**23a–23c**) yielding

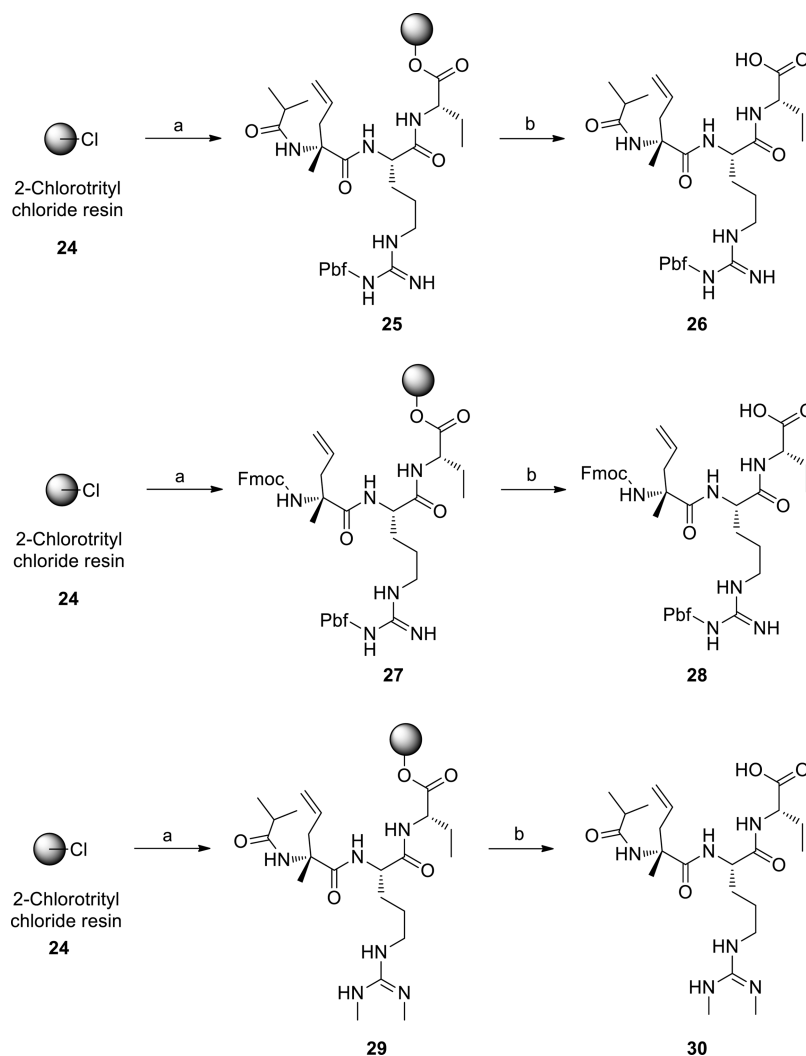
Scheme 1. Fmoc Protection of Unnatural Amino Acids^a

^aReagents and conditions: (a) Fmoc-OSu, DIPEA, dioxane–H₂O (2:1), rt, 5 h.

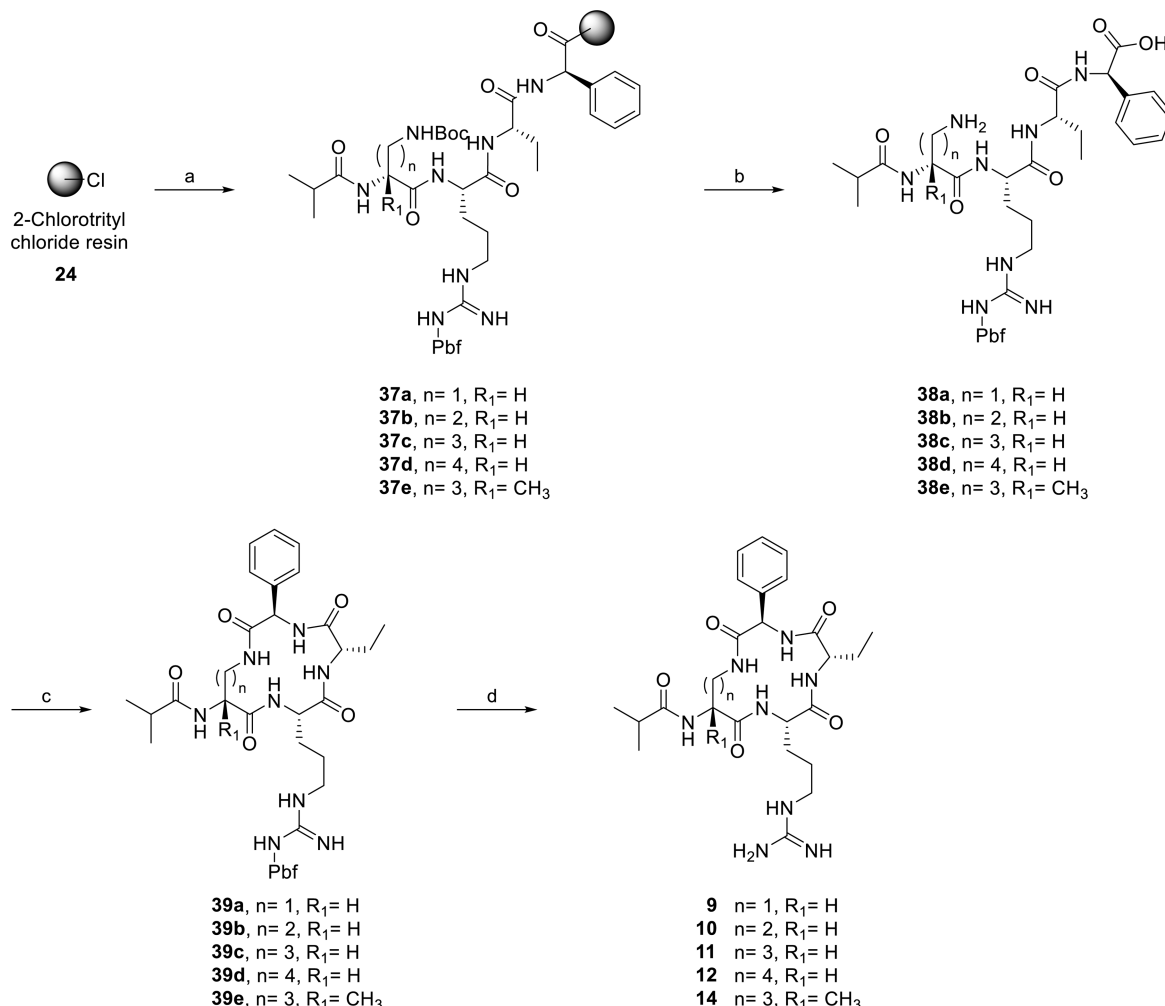
32a–32g. Fmoc protecting group from 32a and 32e was then removed with diethylamine treatment, and the remaining amine was coupled to Fmoc-2-Abu-OH yielding 33a and 33e,

respectively. A similar method used to make 33a and 33e was applied for the synthesis of 34a, 34e, 34h, 35a, 35e, and 35h. Intermediates 35f and 35g were prepared upon Fmoc deprotection of 32f and 32g with diethylamine followed by amide coupling with intermediate 28 synthesized in Scheme 2. Fmoc deprotection of 35a and 35e–35h followed by N-terminal capping with isobutyl chloride afforded 36a and 36e–36h. Fmoc deprotection of 32b–32d followed by amide coupling with intermediate 26 afforded 36b–36d. The same procedure was applied to achieve 36i starting with 32a and carboxylic acid 30. RCM cyclization of 36a–36h followed by catalytic hydrogenation and removal of the Pbf protecting group from arginine side chain yielded the cyclic peptidomimetics 2–6 and 15–17 as trifluoroacetic acid salts. For the synthesis of 7, 36i was subjected to RCM cyclization, followed by catalytic hydrogenation and treatment with acid to obtain 7 as trifluoroacetic acid salt.

Synthesis of cyclic peptidomimetics 9–14, 18, and 19 is shown in Schemes 4 and 5. Intermediates 37a–37e, 41a, and 41b were prepared on the 2-chlorotrityl chloride resin (24) using solid phase peptide synthesis with Fmoc chemistry. The intermediate peptides were cleaved from the resin followed by

Scheme 2. Solid Phase Synthesis of Carboxylic Acid Intermediates^a

^aReagents and conditions: (a) Solid phase peptide synthesis; (b) 1% CF₃COOH in CH₂Cl₂, rt, 30 min.

Scheme 4. Synthesis of Designed Cyclic Peptidomimetics 9–12 and 14^a

^aReagents and conditions: (a) Solid phase peptide synthesis; (b) 1% CF₃COOH in CH₂Cl₂, rt, 30 min then 10% CF₃COOH in CH₂Cl₂ 1 h; (c) HATU, DIPEA, DMF, rt, 1 h; (d) 95% CF₃COOH in water, rt, 2 h.

Boc or Benzyl protecting group removal with 10% trifluoroacetic acid in dichloromethane or hydrogenation with Pd/C in ethanol, respectively, to yield peptides 38a–38e (Scheme 4) and 42a–42c (Scheme 5). Intramolecular amide coupling of 38a–38e and 42a–42c followed by removal of the Pbf protecting group from the arginine side chain yielded cyclic peptidomimetics 9–14, 18, and 19 as trifluoroacetic acid salts.

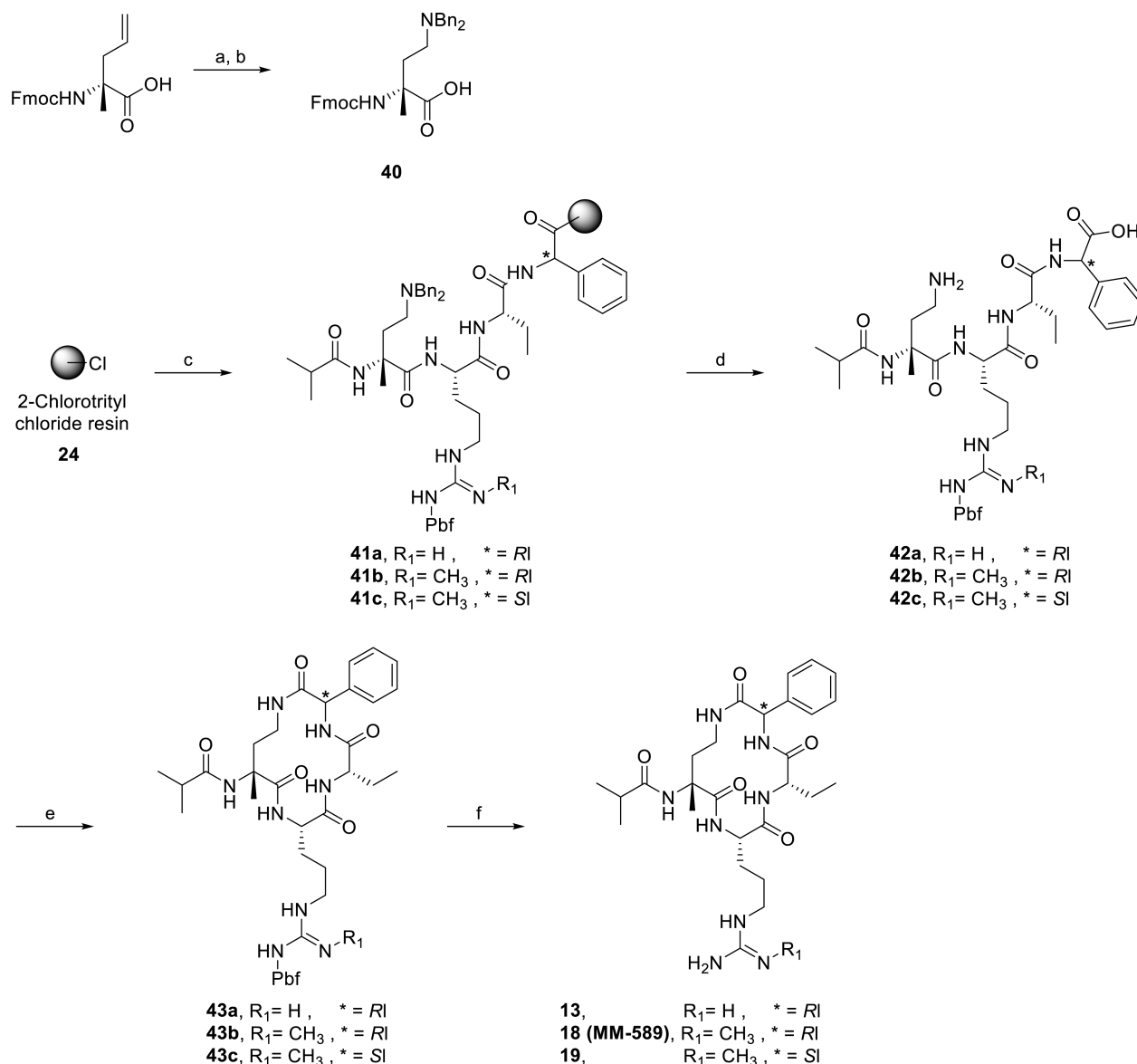
SUMMARY

In the present study, we describe the design, synthesis, and evaluation of macrocyclic peptidomimetics that bind to the MLL binding site in WDR5. This study has determined the optimal linker length in these macrocyclic peptidomimetics and discovered a number of potent and promising macrocyclic peptidomimetics with 18 as the best compound. Compound 18 binds to WDR5 with an IC₅₀ value of 0.90 nM (*K_i* value of <1 nM) and inhibits the MLL HMT activity with an IC₅₀ value of 12.7 nM. Significantly, 18 achieves IC₅₀ values of 0.21 μM and 0.25 μM, respectively, in inhibition of cell growth in the MOLM-13 and MV4-11 human AML cell lines harboring MLL translocation. In comparison, 18 is >40-times more potent than the previously published best compound 2 in inhibition of the MLL HMT activity and growth of MOLM-13 and MV4-11 cell

lines. Furthermore, 18 displays >30-fold selectivity for MOLM-13 and MV4-11 cell lines carrying MLL translocation over HL-60 leukemia cell line lacking MLL translocation. Compound 18 displays excellent metabolic stability in human, mouse, and rat microsomes (*T*_{1/2} > 60 min). Cocystal structures of compounds 16 and 18 in complex with WDR5 provide structural basis for their high binding affinity to WDR5. Compound 18 represents the most potent inhibitor of the WDR5–MLL interaction reported to date. Further optimization of 18 may ultimately yield a new therapy for the treatment of human acute leukemia carrying MLL translocation and potentially other human diseases and conditions that depend upon the MLL HMT activity, the WDR5–MLL interaction, or WDR5.

EXPERIMENTAL SECTION

General. All the final compounds were characterized with ¹H NMR, ¹³C NMR (300 or 400 MHz, Bruker), and HRMS (ESI+) (Agilent Q-TOF Electrospray). The intermediates were characterized with ¹H NMR, ¹³C NMR (300 or 400 MHz, Bruker), and MS (ESI+) (Thermo Scientific LCQ Fleet). Chemical shifts were reported in ppm relative to TMS. D₂O (4.79 ppm), CD₃OD (3.31 ppm), CD₃CN (1.94 ppm), or DMSO-*d*₆ (2.50 ppm) was used as the internal standard for ¹H NMR spectra. D₂O (1,4-dioxane, 66.7 ppm), CD₃OD (49.2 ppm),

Scheme 5. Synthesis of Designed Cyclic Peptidomimetics 13, 18, and 19^a

^aReagents and conditions: (a) OsO_4 , $NaIO_4$, H_2O , THF, rt, 4 h; (b) dibenzylamine, $NaBH(OAc)_3$, $ClCH_2CH_2Cl$, rt, 10 h; (c) solid phase peptide synthesis; (d) 1% CF_3COOH in CH_2Cl_2 , rt, 30 min then H_2 , Pd/C, ethanol, 50 °C, 12 h; (e) HATU, DIPEA, DMF, rt, 1 h; (f) 95% CF_3COOH in water, rt, 2 h.

CD_3CN (1.4 ppm), or $DMSO-d_6$ (39.5 ppm) was used as internal standard for ^{13}C NMR spectra. The final products were purified on a preparative HPLC (Waters 2545, Quaternary Gradient Module) with a SunFire Prep C18 OBD 5 μm , 50 mm \times 100 mm reverse-phase column. The mobile phase was a gradient of solvent A (0.1% trifluoroacetic acid in water) and solvent B (0.1% trifluoroacetic acid in CH_3CN) at a flow rate of 60 mL/min and 1%/min increase of solvent B. All final compounds have purity $\geq 95\%$ as determined by Waters ACQUITY UPLC using reverse-phase column (SunFire, C18, 5 μm , 4.6 mm \times 150 mm) and a solvent gradient of A (0.1% of trifluoroacetic acid in water) and solvent B (0.1% of trifluoroacetic acid in CH_3CN).

Competitive Binding Experiments to WDR5 Protein. The binding affinities of these synthesized compounds were tested using a fluorescence polarization (FP) based competitive binding assay described earlier.¹⁰ Briefly, to a 5 μL solution of the tested compound in DMSO, 120 μL of preincubated complex solution (N-terminal His-tagged WDR5 protein (residues 24–334), named WDR5 Δ 23, and 5-FAM labeled tracer) in assay buffer (0.1 M phosphate, 25 mM KCl,

0.01% Triton, pH 6.5) was added, giving final concentrations of WDR5 Δ 23 and the tracer of 4 nM and 0.6 nM, respectively. The plates were incubated at room temperature on a shaker for 3 h, and then the mP values were measured using the Tecan Infinite M-1000 plate reader (Tecan U.S., Research Triangle Park, NC). K_i values were calculated using the equation described previously.¹⁰

In Vitro Cell-Free MLL HMT Functional Assay. The recombinant MLL complex containing human MLL (MLL1) protein (3735–3973) with N-terminal GST tag and MW = 53.7 kDa, full length human WDR5 with N-terminal 6 \times His tag and MW = 35 kDa, full length human ASH2L with N-terminal 6 \times His tag and MW = 61 kDa, full length human RbbP5 with N-terminal 6 \times His-tag and MW = 60 kDa, and full length human DPY30 with N-terminal 6 \times His-tag and MW = 12 kDa, and recombinant nucleosomes were obtained from Activmotif (Carlsbad, CA). Anti-histone H3 lysine 4 (H3K4me1–2) AlphaLISA acceptor beads, AlphaScreen streptavidin donor beads and biotinylated anti-H3 (C-terminus) antibody were obtained from PerkinElmer Life Sciences (Waltham, MA). Compound serial dilutions (2.5 μL) in assay buffer with 4% DMSO and 5 μL of pentameric MLL

complex solution were added into a white low volume 384 well microtiter plate, which was incubated for 30 min with gentle shaking at room temperature, followed by addition of 2.5 μL of SAM/Nucleosome mixture. The methylation reaction was performed in 50 mM Tris, pH 8.5, with 1 mM DTT and 0.01% Tween-20 added right before the assay. Final concentrations of MLL complex, SAM, and nucleosomes were 5, 200, and 3 nM, respectively. Final DMSO in the reaction mixture was 1%. The reaction was allowed to proceed for 120 min in the dark with gentle shaking at room temperature. Concentrations of reaction components and times were adjusted accordingly for assay development experiments. Five microliters of high salt stopping solution (50 mM Tris, pH 7.4, with 1 M NaCl, 0.1% Tween-20, and 0.3% poly(L-lysine)) was added to stop the methylation reactions for 15 min. Five microliters of 5 \times acceptor beads/biotinylated anti-H3 antibody mixture in detection buffer (50 mM Tris, pH 7.4, with 0.3 M NaCl, 0.1% Tween-20, and 0.001% poly(L-lysine)) was added, followed by 1 h incubation at room temperature to allow full interaction between antibodies and methylated nucleosomes. Then 5 μL of 5 \times streptavidin donor beads was added in detection and incubated for 30 min.

Plates were read on a BMG CLARIOstar microplate reader with an excitation wavelength of 680 nm and emission wavelength of 615 nm. IC₅₀ values of compounds were obtained by fitting the fluorescence intensities detected at 615 nm versus compound concentrations in a sigmoidal dose–response curve (variable slope) with a nonlinear regression, using Graphpad Prism 6.0 software (Graphpad Software, San Diego, CA).

Purification of WDR5 Protein. WDR5 (residues 24–334) was cloned into a His₆-SUMO-vector. The protein was expressed in *Escherichia coli* Rosetta 2 (DE3) cells using Luria Broth media. Cells were subsequently sonicated in 25 mM Tris, pH 8.0, 500 mM NaCl, 5% glycerol, 1 mM benzamidine, 0.1% NP40, and 0.1% β ME with protease inhibitors. The cellular debris was pelleted at 17 000 rpm for 45 min, and the supernatant was loaded onto a Ni-NTA resin (Qiagen) pre-equilibrated with 25 mM Tris, pH 8.0, 500 mM NaCl, 20 mM imidazole, and 5% glycerol. The column was then washed with 25 mM Tris, pH 8.0, 1 M NaCl, and 5% glycerol to remove contaminants, and the protein was eluted with 25 mM Tris, pH 8.0, 150 mM NaCl, 250 mM imidazole, and 5% glycerol. The eluate was incubated with His₆-Ulp1 and dialyzed against 25 mM Tris, pH 8.0, and 150 mM NaCl overnight at 4 $^{\circ}\text{C}$, then applied to fresh Ni-NTA to remove the cleaved tag and protease. The flow through of the Ni-NTA column was loaded onto a Source S column (GE Healthcare) pre-equilibrated with 25 mM Tris, pH 8.0, and 5% glycerol. The protein was eluted with a 0–500 mM NaCl gradient. For crystallographic studies, the protein was then dialyzed against 25 mM Tris, pH 8.0, and 150 mM NaCl overnight at 4 $^{\circ}\text{C}$, concentrated to 20–30 mg/mL, and stored at -80°C .

Crystallization and Structural Determination. WDR5/compound 16 binary complex was obtained by mixing WDR5 and compound 16 at molar ratio 1:2 before crystallization. The complex was crystallized at 25% *tert*-butanol, 0.1 M Tris-HCl, pH 7.5, at 293 K. The crystals were harvested in the same buffer with 20% glycerol. The 2.8 Å data set was collected at Advanced Photon Source beamline 21ID-G and was processed by HKL2000.²⁴ The crystals belong to $P2_12_12_1$ space group. The structure was solved by molecular replacement with Phaser²⁵ using the previously published WDR5 structure (2H14).²⁶ There is one WDR5 molecule in one asymmetric unit. The structure was refined in Phenix²⁷ with manual model building in Coot.²⁸ The final model has good stereochemistry with an R -value of 19.0% and an R_{free} of 24.7%.

The WDR5–18 complex was formed by diluting the protein to 7 mg/mL with 50 mM Bis-Tris, pH 6.5, and 150 mM NaCl, then incubating with 18 in a 1:1.1 molar ratio for 1 h at 4 $^{\circ}\text{C}$. Crystals formed at 20 $^{\circ}\text{C}$ in drops containing equal volumes of protein solution and precipitant (0.1 M Na Bis-Tris, pH 6.5, 26% PEG 8000, and 0.1 M ammonium sulfate). The crystals were cryoprotected with well solution containing 20% ethylene glycol. Diffraction data were collected at 0.9787 Å wavelength on a Rayonix – MX300 detector at LS-CAT 21-ID-F beamline at the Advanced Photon Source, then

processed with HKL2000.²⁴ WDR5 in complex with compound 18 crystallized in C2 space group with 1 molecule of WDR5 per asymmetric unit. The structure was solved to 1.64 Å via molecular replacement²⁹ with WDR5 (PDB ID 3SMR) as the search model. Iterative rounds of electron density fitting and refinement were completed using Coot²⁸ and BUSTER,³⁰ respectively. The coordinates and geometric restraints for each compound were created from smiles using grade³⁰ with the *qm+mogul* option. The first seven residues are disordered in all the structures. Data collection and refinement statistics are shown in Table S1.

Cell Viability Assay of Leukemia Cells. To assess cell viability (Tables 2 and 5), MOLM-13 leukemia cells carrying MLL-AF9 fusion, MV4-11 leukemia cells carrying MLL-AF4 fusion, or HL-60 leukemia cells carrying no MLL fusion were seeded 1×10^4 cells/well in 96-well plates and treated with an inhibitor for 4 days at different concentrations, in culture media containing 0.2% DMSO as the final concentration. Cell viability was determined using the WST-8 cell proliferation assay kit (Dojindo Molecular Technologies) according to manufacturer's instructions. Three independent experiments in triplicate were performed. Data were analyzed using Prism software to determine 50% of cell growth inhibition (IC₅₀) values versus DMSO control.

To assess the effect of long-term treatment of compound 18 on leukemia cells (Figure 5), MOLM-13 and MV4-11 cell lines were plated at a density of 5×10^4 cell/mL in 24-well plates (2 mL/well) and treated with the relevant concentrations. On day 4, cell viability for each treatment was measured using the WST-8 cell count kit. Then 10% of viable cells from each well were transferred to freshly prepared medium containing corresponding concentrations of compound 18 and cultured for additional 3 days. On day 7, cell viability for each treatment was determined.

Computational Docking. Docking studies were performed using the previously reported structure of WDR5 in complex with 1 (PDB ID 4GM3) with the GOLD^{31,32} program (version 5.2) with the Arg moiety of compound 1 serving as a scaffold for constrained docking. For each genetic algorithm (GA) run, a maximum number of 200 000 operations were performed on a population of five islands of 100 individuals. Operator weights for crossover, mutation, and migration were set to 95, 95, and 10, respectively. The docking simulations were terminated after 10 runs for each ligand, using the Goldscore fitness function to evaluate the docked conformations. The top 10 conformations were saved for analysis of the predicted docking modes.

Chemical Synthesis Procedures, NMR Spectra, and HRMS Data of the Representative Compounds. *Method A.* The Fmoc protected intermediate was treated with diethylamine (20 equiv) in CH₃CN for 2 h at room temperature followed by removal of the solvent and diethylamine in vacuo. The resulting crude was further dried under vacuum, then taken into CH₂Cl₂ and mixed with the corresponding Fmoc-amino acid or peptide carboxylic acid (1.5 equiv), EDCI (1.5 equiv), HOAt (1.5 equiv), and diisopropylethylamine (1.5 equiv). The reaction mixture was stirred at room temperature for 2–3 h, quenched with H₂O and extracted to CH₂Cl₂. The organic layers were collected and dried over anhydrous Na₂SO₄, filtered, evaporated, and purified over flash chromatography.

Method B. To a solution of intermediate 36a–36h in CH₂Cl₂, Hoveyda–Grubbs second generation catalyst (0.5 equiv) was added under N₂ atmosphere, and the reaction mixture was stirred at 45 $^{\circ}\text{C}$ overnight under N₂ atmosphere unless stated otherwise. With intermediates 36e–36g, another portion of the catalyst (0.5 equiv) was added and stirred further overnight under the same conditions before filtering through Celite and concentrating in vacuo. The remaining crude was purified over flash chromatography using CH₂Cl₂/MeOH. The cyclic product was taken up in MeOH, and the double bond was reduced using 10% Pd/C under 1 atm of H₂. The reaction mixture was filtered through Celite and concentrated. The remaining crude was refluxed in CH₂Cl₂/trifluoroacetic acid/H₂O (20:10:0.5) for 2 h in order to remove the Pbf group from arginine guanidine and evaporated. The crude product was purified with preparative HPLC using the C18 reverse phase column (Waters,

Sunfire Prep C₁₈ OBD, 5 μm, 50 mm × 100 mm). The final compound then dissolved in CH₃CN/H₂O (1:1) and lyophilized.

N-((3*R*,6*S*,9*S*,12*R*)-6-Ethyl-9-(3-guanidinopropyl)-12-methyl-2,5,8,11-tetraoxo-3-phenyl-1,4,7,10-tetraazacyclohexadecan-12-yl)isobutyramide CF₃COOH Salt (**2**). Compound **2** was prepared according Method B starting from **36a**. The RCM cyclization was achieved at room temperature overnight. White solid (53% yield over 3 steps). HRMS (ESI⁺): *m/z* calcd for C₂₉H₄₇N₈O₅ [M + H]⁺ 587.3664, found 587.3664. ¹H NMR (300 MHz, MeOD): δ 7.42–7.30 (m, 5H), 5.25 (s, 1H), 4.30 (dd, *J* = 4.2, 9.8 Hz, 1H), 4.16 (dd, *J* = 6.2, 7.7 Hz, 1H), 3.51–3.42 (m, 1H), 3.19 (t, *J* = 6.9 Hz, 2H), 3.12–2.99 (m, 1H), 2.59–2.48 (m, 1H), 1.94–1.26 (m, 15H), 1.15–1.08 (m, 6H), 0.92 (t, *J* = 7.4 Hz, 3H). ¹³C NMR (75 MHz, MeOD-*d*₄): δ 179.86, 176.83, 174.99, 173.64, 172.97, 158.86, 137.93, 130.06, 129.69, 129.32, 61.24, 60.70, 56.67, 55.27, 41.91, 40.34, 39.25, 36.12, 29.99, 26.39, 25.94, 22.81, 21.83, 20.06, 19.91, 10.84.

N-((3*R*,6*S*,9*S*,12*R*)-6-Ethyl-9-(3-guanidinopropyl)-1,12-dimethyl-2,5,8,11-tetraoxo-3-phenyl-1,4,7,10-tetraazacyclohexadecan-12-yl)isobutyramide CF₃COOH Salt (**3**). The compound was prepared according Method B starting from **36e**. White solid (18% yield over 3 steps). HRMS (ESI): *m/z* calcd for C₃₀H₄₉N₈O₅ [M + H]⁺ 601.3820, found 601.3819. ¹H NMR (300 MHz, CD₃OD, rotamers) δ: 7.41–7.21 (m, 5H), 5.91 (s, 1H), 4.28–4.20 (m, 1H), 4.10 (dd, *J* = 4.7, 10.1 Hz, 1H), 3.21 (t, *J* = 7.1 Hz, 2H), 3.01 (s, 2.6H), 2.95 (s, 0.4H), 2.84–2.72 (m, 1H), 2.62–2.51 (m, 1H), 2.07–1.21 (m, 16H), 1.18–1.08 (m, 6H), 1.00 (t, *J* = 7.3 Hz, 2.4H), 0.91 (t, *J* = 7.3 Hz, 0.6H). ¹³C NMR (75 MHz, CD₃OD, rotamers) δ: 180.14, 176.79, 174.99, 173.94, 172.30, 158.88, 138.57, 129.49, 129.28, 128.95, 60.76, 57.29, 56.26, 56.00, 47.38, 42.01, 40.82, 36.21, 35.54, 29.60, 27.91, 26.38, 25.61, 25.50, 21.67, 20.58, 19.72, 17.73.

N-((3*R*,6*S*,9*S*,12*R*)-6-Ethyl-3-(4-fluorophenyl)-9-(3-guanidinopropyl)-1,12-dimethyl-2,5,8,11-tetraoxo-1,4,7,10-tetraazacyclohexadecan-12-yl)isobutyramide CF₃COOH Salt (**4**). The compound was synthesized using Method B starting from **36f**. White solid (11% yield over 3 steps). HRMS (ESI): *m/z* calculated for C₃₀H₄₈FN₈O₅ [M + H]⁺ 619.3726, found 619.3731. ¹H NMR (300 MHz, CD₃OD, 2-rotamers) δ: 7.44–7.36 (m, 2H), 7.16–7.00 (m, 2H), 5.94 (s, 1H), 4.24–4.16 (m, 1H), 4.07 (dd, *J* = 4.2, 10.5 Hz, 1H), 3.20 (t, *J* = 7.1 Hz, 2H), 2.99 (s, 2.5H), 2.93 (s, 0.5 Hz), 2.78–2.68 (m, 1H), 2.63–2.49 (m, 1H), 2.14–1.18 (m, 16H), 1.15 (d, *J* = 6.8 Hz, 3H), 1.11 (d, *J* = 6.7 Hz, 3H), 1.01 (t, *J* = 7.3 Hz, 2.5H), 0.89 (t, *J* = 7.4 Hz, 0.5H). ¹³C NMR (75 MHz, CD₃OD) δ: 180.14, 177.04, 175.19, 174.05, 172.07, 158.88, 134.96, 134.93, 131.36, 131.26, 116.12, 115.83, 60.69, 57.55, 56.61, 55.15, 46.99, 42.01, 40.67, 36.21, 35.29, 29.36, 27.51, 26.43, 26.16, 25.44, 21.54, 20.72, 19.63, 11.89.

N-((3*R*,6*S*,9*S*,12*R*)-3-(4-Chlorophenyl)-6-ethyl-9-(3-guanidinopropyl)-1,12-dimethyl-2,5,8,11-tetraoxo-1,4,7,10-tetraazacyclohexadecan-12-yl)isobutyramide CF₃COOH Salt (**5**). The compound was synthesized using Method B starting from **36g**. Ph₂S was added during catalytic hydrogenation in order to reduce the activity of Pd/C. White solid (11% yield over 3 steps). HRMS (ESI): *m/z* calculated for C₃₀H₄₈ClN₈O₅ [M + H]⁺ 635.3431, found 635.3428. ¹H NMR (300 MHz, CD₃OD, rotamers) δ: 7.41–7.29 (m, 4H), 5.95 (s, 1H), 4.20 (t, 1H, *J* = 6.6 Hz), 4.07 (dd, 1H, *J* = 4.2, 10.4 Hz), 3.25–3.17 (m, 2H), 2.99 (s, 2.4H), 2.94 (s, 0.4 H), 2.90 (s, 0.2H), 2.77–2.68 (m, 1H), 2.62–2.51 (m, 1H), 2.15–1.59 (m, 9H), 1.55–1.18 (m, 7H), 1.16 (d, 3H, *J* = 6.8 Hz), 1.12 (d, 3H, *J* = 6.7 Hz), 1.02 (t, *J* = 7.4 Hz, 2.3 H), 0.90 (t, *J* = 7.5 Hz, 0.7 H). ¹³C NMR (75 MHz, CD₃OD) δ: 180.13, 177.03, 175.22, 174.10, 171.85, 158.89, 137.86, 134.64, 131.07, 129.38, 60.68, 57.64, 56.59, 55.23, 46.88, 42.01, 40.69, 36.23, 35.25, 29.35, 27.43, 26.43, 26.29, 25.41, 21.51, 20.75, 19.61, 11.92.

N-((3*R*,6*S*,9*S*,12*R*)-6-Ethyl-12-methyl-9-(3-(3-methylguanidino)propyl)-2,5,8,11-tetraoxo-3-phenyl-1,4,7,10-tetraazacyclohexadecan-12-yl)isobutyramide CF₃COOH Salt (**6**). The compound was synthesized using Method B starting from **36h**. The RCM cyclization was achieved at room temperature overnight. White solid (75% yield over 3 steps). HRMS (ESI): *m/z* calculated for C₃₀H₄₉N₈O₅ [M + H]⁺ 601.3820, found 601.3829. ¹H NMR (300 MHz, CD₃OD) δ: 7.42–7.33 (m, 5H), 5.24 (s, 1H), 4.30 (dd, *J* = 4.2, 9.8 Hz, 1H), 4.17 (dd, *J* = 6.0, 7.8 Hz, 1H), 3.52–3.43 (m, 1H), 3.18 (t, *J* = 6.9 Hz, 2H), 3.11–2.99 (m, 1H), 2.85 (s, 3H), 2.59–2.48 (m, 1H), 1.96–1.24 (m, 15H),

1.18–1.06 (m, 6H), 0.92 (t, *J* = 7.5 Hz, 3H). ¹³C NMR (75 MHz, CD₃OD) δ: 179.84, 176.79, 175.01, 173.94, 172.98, 158.42, 137.90, 130.06, 129.70, 129.33, 61.29, 60.68, 56.62, 55.22, 41.93, 40.39, 39.28, 36.11, 30.06, 28.54, 26.40, 25.98, 22.79, 21.86, 20.08, 19.90, 10.81.

N-((3*R*,6*S*,9*S*,12*R*)-9-(3-((*E*)-2,3-dimethylguanidino)propyl)-6-ethyl-12-methyl-2,5,8,11-tetraoxo-3-phenyl-1,4,7,10-tetraazacyclohexadecan-12-yl)isobutyramide CF₃COOH Salt (**7**). The compound was synthesized according to Method B starting from **36i** with the following modification. The RCM cyclization was achieved at room temperature overnight. After the catalytic hydrogenation step, the crude was taken into CH₂Cl₂/trifluoroacetic acid (1:1) and stirred for 0.5 h at room temperature in order to form the trifluoroacetic acid salt. This mixture was evaporated and purified. White solid (27% yield over 3 steps). HRMS (ESI): *m/z* calculated for C₃₁H₅₁N₈O₅ [M + H]⁺ 615.3977, found 615.3975. ¹H NMR (300 MHz, CD₃OD) δ: 7.42–7.33 (m, 5H), 5.24 (s, 1H), 4.36–4.28 (m, 1H), 4.18 (dd, *J* = 6.0, 7.8 Hz, 1H), 3.53–3.43 (m, 1H), 3.20 (t, *J* = 7.0 Hz, 2H), 3.10–2.98 (m, 1H), 2.85 (s, 6H), 2.59–2.48 (m, 1H), 1.96–1.23 (m, 15H), 1.15–1.07 (m, 6H), 0.92 (t, *J* = 7.4 Hz, 3H). ¹³C NMR (75 MHz, CD₃OD) δ: 179.79, 176.72, 175.06, 173.95, 172.97, 157.53, 137.88, 130.06, 129.71, 129.32, 61.34, 60.66, 56.56, 55.17, 41.93, 40.41, 39.29, 36.10, 30.06, 28.52, 26.34, 26.01, 22.89, 21.91, 20.07, 19.91, 10.81.

N-((3*S*,6*R*,9*R*,12*S*)-6-Ethyl-9-(3-guanidinopropyl)-12-methyl-2,5,8,11-tetraoxo-3-phenyl-1,4,7,10-tetraazacyclohexadecan-12-yl)isobutyramide CF₃COOH Salt (**8**, MM-NC-401). The procedure, used to make **2**, was applied for making **8**. Identical NMR spectrum and ESI-MS data were observed.

N-((3*R*,6*S*,9*S*,12*R*)-6-Ethyl-9-(3-guanidinopropyl)-2,5,8,11-tetraoxo-3-phenyl-1,4,7,10-tetraazacyclotridecan-12-yl)isobutyramide CF₃COOH Salt (**9**). A method applied for **12** was used to make **9** starting from **24**. White solid (24.5% yield over 4 steps). HRMS (ESI): *m/z* calculated for C₂₅H₃₉N₈O₅ [M + H]⁺ 531.3038, found 531.3040. ¹H NMR (400 MHz, DMSO-*d*₆) δ 7.47–7.12 (m, 5H), 5.29 (s, 1H), 4.36 (t, *J* = 4.4 Hz, 1H), 4.10 (t, *J* = 7.8 Hz, 1H), 4.04 (t, *J* = 7.5 Hz, 1H), 3.58 (dd, *J* = 13.8, 4.4 Hz, 1H), 3.34 (dd, *J* = 13.6, 4.7 Hz, 1H), 3.12–2.93 (m, 2H), 2.48–2.41 (m, 1H), 1.80–1.29 (m, 6H), 1.03 (d, *J* = 2.6 Hz, 3H), 1.01 (d, *J* = 2.7 Hz, 3H), 0.77 (t, *J* = 7.4 Hz, 3H). ¹³C NMR (75 MHz, DMSO) δ 176.36, 172.67, 171.06, 170.69, 170.63, 156.74, 137.19, 128.18, 127.59, 127.55, 57.49, 55.18, 54.67, 53.39, 40.78, 34.24, 27.40, 25.31, 23.21, 19.48, 19.09, 10.54.

N-((3*R*,6*S*,9*S*,12*R*)-6-Ethyl-9-(3-guanidinopropyl)-2,5,8,11-tetraoxo-3-phenyl-1,4,7,10-tetraazacyclotetradecan-12-yl)isobutyramide CF₃COOH Salt (**10**). A method applied for **12** was used to make **10** starting from **24**. White solid (21.7% yield over 4 steps). HRMS (ESI): *m/z* calculated for C₂₆H₄₁N₈O₅ [M + H]⁺ 545.3200, found 545.3197. ¹H NMR (400 MHz, CD₃OD) δ 7.44–7.36 (m, 2H), 7.36–7.26 (m, 3H), 5.44 (s, 1H), 4.33–4.21 (m, 2H), 4.18 (dd, *J* = 7.7, 6.2 Hz, 1H), 3.68 (dt, *J* = 14.4, 3.7 Hz, 1H), 3.26–3.10 (m, 2H), 2.88 (dd, *J* = 14.3, 11.8 Hz, 1H), 2.65 (hept, *J* = 6.6 Hz, 1H), 2.55–2.39 (m, 1H), 2.22–2.03 (m, 1H), 1.89–1.59 (m, 6H), 1.19 (dd, *J* = 13.8, 6.8 Hz, 6H), 0.94 (t, *J* = 7.4 Hz, 3H). ¹³C NMR (101 MHz, CD₃OD) δ 181.84, 175.27, 175.05, 172.50, 172.27, 158.65, 139.13, 129.49, 129.39, 128.96, 58.55, 57.07, 55.76, 54.13, 41.74, 36.09, 35.68, 30.21, 28.78, 26.53, 24.52, 20.38, 19.42, 11.07.

N-((3*R*,6*S*,9*S*,12*R*)-6-Ethyl-9-(3-guanidinopropyl)-2,5,8,11-tetraoxo-3-phenyl-1,4,7,10-tetraazacyclopentadecan-12-yl)isobutyramide CF₃COOH Salt (**11**). A method applied for **12** was used to make **11** starting from **24**. White solid (21.5% yield over 4 steps). HRMS (ESI): *m/z* calculated for C₂₇H₄₃N₈O₅ [M + H]⁺ 559.3356, found 559.3351. ¹H NMR (400 MHz, CD₃OD) δ 7.47–7.25 (m, 5H), 5.27 (s, 1H), 4.31 (dd, *J* = 10.5, 5.0 Hz, 1H), 4.20 (dd, *J* = 7.9, 6.4 Hz, 1H), 3.96 (dd, *J* = 9.5, 3.7 Hz, 1H), 3.46–3.37 (m, 1H), 3.24–3.01 (m, 3H), 2.65–2.49 (m, 1H), 1.93–1.60 (m, 10H), 1.15 (dd, *J* = 6.9, 5.9 Hz, 6H), 0.93 (t, *J* = 7.5 Hz, 3H). ¹³C NMR (101 MHz, CD₃OD) δ 180.68, 175.30, 174.76, 173.75, 172.98, 158.61, 137.32, 129.90, 129.58, 129.22, 60.94, 56.96, 56.23, 55.33, 41.56, 39.56, 35.76, 29.84, 28.93, 26.58, 26.15, 19.96, 19.63, 10.67.

N-((3*R*,6*S*,9*S*,12*R*)-6-Ethyl-9-(3-guanidinopropyl)-2,5,8,11-tetraoxo-3-phenyl-1,4,7,10-tetraazacyclohexadecan-12-yl)isobutyramide CF₃COOH Salt (**12**). Fmoc-D-Phg-OH (0.5 mmol, 0.17 g) was loaded on the 0.1 mmol 2-chlorotriethyl chloride (**24**) resin

(ChemPep) (1 mmol/g) overnight in CH_2Cl_2 and in the presence of 2,4,6-collidine (3 mmol, 0.4 mL). Then, the resin was washed with DMF, MeOH, and CH_2Cl_2 , successively, mixed with DIPEA (0.29 mmol, 0.5 mL) in MeOH/ CH_2Cl_2 (1:5) and shaken for 30 min to end-cap unreacted 2-chlorotrityl groups on the resin. Next, classical chain elongation was carried out with Fmoc chemistry. The peptide intermediate (**38d**) was cleaved from the resin by treatment of **37d** with 4 mL of 1% trifluoroacetic acid in CH_2Cl_2 (3×10 min). The filtrate was evaporated, followed by treatment with 10% trifluoroacetic acid in CH_2Cl_2 for 30 min. Then the solvent was evaporated, and the remaining crude was purified with preparative HPLC using the C18 reverse phase column (Waters, Sunfire Prep C₁₈ OBD, 5 μm , 50 mm \times 100 mm) to yield **38d**. White powder, MS (ESI): m/z calculated for $\text{C}_{41}\text{H}_{63}\text{N}_8\text{O}_9\text{S} [\text{M} + \text{H}]^+$ 843.44, found 843.38.

Intermediate **38d** (50 mg, 0.05 mmol) dissolved in 5 mL of DMF was slowly added to a solution of HATU (38 mg, 0.1 mmol) and DIPEA (0.05 mL, 0.25 mmol) in 5 mL of DMF during 30 min. The reaction was stirred for another 30 min, and then the solvent was evaporated. The remaining crude was purified with preparative HPLC using the C18 reverse phase column (Waters, Sunfire Prep C₁₈ OBD, 5 μm , 50 mm \times 100 mm) to yield **39d**. White powder, MS (ESI): m/z calculated for $\text{C}_{41}\text{H}_{61}\text{N}_8\text{O}_8\text{S} [\text{M} + \text{H}]^+$ 825.43, found 825.36.

The cyclic product **39d** was then dissolved in trifluoroacetic acid/ H_2O (95:5) and stirred at room temperature for 2 h in order to remove the Pbf group from arginine guanidine. Then the solvent was evaporated, and the crude product was purified with preparative HPLC using the C18 reverse phase column (Waters, Sunfire Prep C₁₈ OBD, 5 μm , 50 mm \times 100 mm). The final compound **12** then was dissolved in $\text{CH}_3\text{CN}/\text{H}_2\text{O}$ (1:1) and lyophilized. White solid (12.7% yield over 4 steps). HRMS (ESI): m/z calculated for $\text{C}_{28}\text{H}_{45}\text{N}_8\text{O}_5 [\text{M} + \text{H}]^+$ 573.3513, found 573.3507. ^1H NMR (400 MHz, CD_3OD) δ 7.50–7.28 (m, 5H), 5.14 (s, 1H), 4.28 (t, $J = 6.8$ Hz, 1H), 4.13 (dd, $J = 10.4$, 5.2 Hz, 1H), 4.08–3.99 (m, 1H), 3.54–3.41 (m, 1H), 3.18 (td, $J = 7.1$, 2.5 Hz, 2H), 3.04–2.97 (m, 1H), 2.62–2.51 (m, 1H), 1.94–1.54 (m, 9H), 1.47–1.24 (m, 3H), 1.13 (dd, $J = 6.9$, 3.3 Hz, 6H), 0.90 (t, $J = 7.5$ Hz, 3H). ^{13}C NMR (101 MHz, CD_3OD) δ 180.51, 175.63, 174.34, 173.64, 172.92, 158.63, 137.30, 129.92, 129.67, 129.31, 61.54, 57.09, 56.08, 55.83, 41.61, 39.68, 35.72, 32.14, 29.95, 29.24, 26.68, 26.53, 23.37, 19.93, 19.74, 10.25.

N-((3*R*,6*S*,9*S*,12*R*)-6-Ethyl-9-(3-guanidinopropyl)-12-methyl-2,5,8,11-tetraoxo-3-phenyl-1,4,7,10-tetraazacyclotetradecan-12-yl)isobutyramide CF_3COOH Salt (**13**). Fmoc-D-Phe-OH (0.5 mmol, 0.17 g) was loaded on the 0.1 mmol 2-chlorotrityl chloride (**24**) resin (ChemPep) (1 mmol/g) overnight in CH_2Cl_2 and in the presence of 2,4,6-collidine (3 mmol, 0.4 mL). Then, the resin was washed with DMF, MeOH, and CH_2Cl_2 , successively, mixed with DIPEA (0.29 mmol, 0.5 mL) in MeOH/ CH_2Cl_2 (1:5), and shaken for 30 min to end-cap unreacted 2-chlorotrityl group on the resin. Next, classical chain elongation was carried out with Fmoc chemistry. The peptide intermediate was cleaved from the resin by treatment of **41a** with 4 mL of 1% trifluoroacetic acid in CH_2Cl_2 (3×10 min). The filtrate was evaporated, and the residue was dissolved in anhydrous ethanol. Pd/C (20 mg) was added to the flask, and the reaction was stirred at H_2 atmosphere for 12 h at 50 $^\circ\text{C}$. Then the reaction was filtered, the filtrate was evaporated, and the remaining crude was purified with preparative HPLC using the C18 reverse phase column (Waters, Sunfire Prep C₁₈ OBD, 5 μm , 50 mm \times 100 mm) to yield **42a**. White powder, MS (ESI): m/z calculated for $\text{C}_{40}\text{H}_{61}\text{N}_8\text{O}_9\text{S} [\text{M} + \text{H}]^+$ 829.43, found 829.25.

Then the method applied for **12** starting from **38d** was used to make **13** starting from **42a**. White solid (8.7% yield over 4 steps). HRMS (ESI): m/z calculated for $\text{C}_{27}\text{H}_{43}\text{N}_8\text{O}_5 [\text{M} + \text{H}]^+$ 559.3352, found 559.3351. ^1H NMR (400 MHz, methanol- d_4) δ 7.49–7.37 (m, 2H), 7.37–7.20 (m, 3H), 5.46 (d, $J = 9.2$ Hz, 1H), 4.38 (dd, $J = 10.5$, 3.8 Hz, 1H), 4.24–4.06 (m, 1H), 3.85–3.63 (m, 1H), 3.26–3.16 (m, 2H), 2.76–2.56 (m, 3H), 2.24–2.07 (m, 1H), 1.92–1.59 (m, 5H), 1.53 (s, 3H), 1.40–1.32 (m, 1H), 1.23 (d, $J = 6.9$ Hz, 3H), 1.16 (d, $J = 6.7$ Hz, 3H), 0.96 (t, $J = 7.4$ Hz, 3H). ^{13}C NMR (101 MHz, MeOD) δ 182.07, 177.62, 175.47, 172.28, 172.11, 158.66, 139.36, 129.48, 129.42,

128.86, 59.98, 58.21, 57.51, 55.53, 41.72, 38.63, 36.40, 35.98, 28.83, 26.67, 24.75, 21.17, 18.90, 11.06.

N-((3*R*,6*S*,9*S*,12*R*)-6-Ethyl-9-(3-guanidinopropyl)-12-methyl-2,5,8,11-tetraoxo-3-phenyl-1,4,7,10-tetraazacyclotetradecan-12-yl)isobutyramide CF_3COOH Salt (**14**). A method applied for **12** was used to make **14** starting from **24**. White solid (19.4% yield over 4 steps). HRMS (ESI): m/z calculated for $\text{C}_{28}\text{H}_{45}\text{N}_8\text{O}_5 [\text{M} + \text{H}]^+$ 573.3513, found 573.3506. ^1H NMR (400 MHz, CD_3OD) δ 7.55–7.23 (m, 5H), 5.35 (s, 1H), 4.40 (dd, $J = 10.0$, 4.7 Hz, 1H), 4.16 (dd, $J = 8.6$, 6.3 Hz, 1H), 3.41–3.33 (m, 1H), 3.24–3.12 (m, 3H), 2.65–2.37 (m, 1H), 2.00–1.48 (m, 10H), 1.46 (s, 3H), 1.12 (dd, $J = 6.8$, 2.5 Hz, 6H), 0.94 (t, $J = 7.4$ Hz, 3H). ^{13}C NMR (101 MHz, CD_3OD) δ 179.91, 176.79, 174.82, 174.33, 172.75, 158.62, 138.00, 129.82, 129.37, 128.93, 60.47, 60.37, 56.91, 55.12, 41.74, 40.12, 37.57, 35.81, 28.76, 26.24, 25.14, 23.68, 21.04, 19.97, 19.36, 11.00.

N-((3*R*,6*S*,9*S*,12*R*)-6-Ethyl-9-(3-guanidinopropyl)-12-methyl-2,5,8,11-tetraoxo-3-phenyl-1,4,7,10-tetraazacycloheptadecan-12-yl)isobutyramide CF_3COOH Salt (**15**). Compound **15** was prepared according Method B starting from **36b**. The RCM cyclization was achieved at room temperature overnight. White solid (28% yield over 3 steps). HRMS (ESI): m/z calcd for $\text{C}_{30}\text{H}_{49}\text{N}_8\text{O}_5 [\text{M} + \text{H}]^+$ 601.3820, found 601.3827. ^1H NMR (300 MHz, CD_3OD) δ : 7.45–7.32 (m, 5H), 5.22 (s, 1H), 4.45–4.31 (m, 2H), 3.28–3.13 (m, 4H), 2.59–2.49 (m, 1H), 1.97–1.05 (m, 23H), 0.89 (t, $J = 7.5$ Hz, 3H). ^{13}C NMR (75 MHz, CD_3OD) δ : 179.80, 176.66, 174.54, 173.62, 173.32, 158.81, 137.54, 130.08, 129.79, 129.44, 61.04, 60.91, 55.74, 54.59, 41.83, 41.69, 39.95, 36.05, 30.64, 29.75, 27.18, 27.10, 26.14, 25.08, 21.12, 20.33, 19.48, 10.18.

N-((3*R*,6*S*,9*S*,12*R*)-6-Ethyl-9-(3-guanidinopropyl)-12-methyl-2,5,8,11-tetraoxo-3-phenyl-1,4,7,10-tetraazacyclooctadecan-12-yl)isobutyramide CF_3COOH Salt (**16**). Compound **16** was prepared according Method B starting from **36c**. The RCM cyclization was achieved at room temperature overnight. White solid (46% yield over 3 steps). HRMS (ESI): m/z calcd for $\text{C}_{31}\text{H}_{51}\text{N}_8\text{O}_5 [\text{M} + \text{H}]^+$ 615.3977, found 615.3976. ^1H NMR (300 MHz, CD_3OD) δ : 7.45–7.29 (m, 5H), 5.40 (s, 1H), 4.29–4.19 (m, 2H), 3.59–3.47 (m, 1H), 3.19 (t, $J = 6.7$ Hz, 2H), 3.09–2.96 (m, 1H), 2.63–2.52 (m, 1H), 2.02–1.59 (m, 8H), 1.58–1.27 (m, 11H), 1.14 (d, $J = 6.5$ Hz, 3H), 1.12 (d, $J = 6.5$ Hz, 3H), 0.89 (t, $J = 7.4$ Hz, 3H). ^{13}C NMR (75 MHz, CD_3OD) δ : 180.53, 177.59, 174.48, 173.99, 172.88, 158.86, 138.38, 129.97, 129.57, 60.67, 59.87, 56.51, 55.22, 42.04, 39.80, 37.53, 36.09, 29.98, 28.42, 28.38, 26.42, 25.37, 22.72, 22.47, 20.08, 19.94, 10.69.

N-((3*R*,6*S*,9*S*,12*R*)-6-Ethyl-9-(3-guanidinopropyl)-12-methyl-2,5,8,11-tetraoxo-3-phenyl-1,4,7,10-tetraazacycloicosan-12-yl)isobutyramide CF_3COOH Salt (**17**). Compound **17** was prepared according Method B starting from **36d**. The RCM cyclization was achieved at room temperature overnight. White solid (27% yield over 3 steps). HRMS (ESI): m/z calcd for $\text{C}_{33}\text{H}_{55}\text{N}_8\text{O}_5 [\text{M} + \text{H}]^+$ 643.4290, found 643.4292. ^1H NMR (300 MHz, CD_3OD) δ : 7.41–7.30 (m, 5H), 5.40 (s, 1H), 4.34–4.28 (m, 1H), 4.18 (t, $J = 7.1$ Hz, 1H), 3.55–3.44 (m, 1H), 3.17 (t, $J = 6.9$ Hz, 2H), 3.07–2.95 (m, 1H), 2.61–2.50 (m, 1H), 2.00–1.28 (m, 23H), 1.16–1.07 (m, 6H), 0.92 (t, $J = 7.4$ Hz, 3H). ^{13}C NMR (75 MHz, CD_3OD) δ : 180.22, 176.92, 174.53, 174.30, 172.69, 158.81, 138.70, 130.03, 129.55, 129.39, 60.72, 59.51, 57.11, 54.55, 42.14, 40.03, 38.56, 36.13, 30.28, 29.31, 28.92, 28.63, 28.04, 26.56, 26.16, 26.10, 23.50, 22.76, 20.05, 10.81.

N-((3*R*,6*S*,9*S*,12*R*)-6-Ethyl-12-methyl-9-(3-(3-methylguanidino)propyl)-2,5,8,11-tetraoxo-3-phenyl-1,4,7,10-tetraazacyclotetradecan-12-yl)isobutyramide CF_3COOH Salt (**18**). A method applied for **13** was used to make **18** starting from **24**. White solid (15.4% yield over 4 steps). HRMS (ESI): m/z calculated for $\text{C}_{28}\text{H}_{45}\text{N}_8\text{O}_5 [\text{M} + \text{H}]^+$ 573.3507, found 573.3511. ^1H NMR (400 MHz, methanol- d_4) δ 7.44–7.37 (m, 2H), 7.37–7.26 (m, 3H), 5.48–5.44 (m, 1H), 4.38 (dd, $J = 10.5$, 3.7 Hz, 1H), 4.17 (td, $J = 7.0$, 3.2 Hz, 1H), 3.80–3.72 (m, 1H), 3.28–3.16 (m, 2H), 2.83 (s, 3H), 2.75–2.57 (m, 3H), 2.25–2.11 (m, 1H), 1.96–1.69 (m, 4H), 1.53 (s, 3H), 1.41–1.32 (m, 1H), 1.22 (d, $J = 6.9$ Hz, 3H), 1.16 (d, $J = 6.7$ Hz, 3H), 0.95 (t, $J = 7.4$ Hz, 3H). ^{13}C NMR (101 MHz, MeOD) δ 182.17, 177.63, 175.52, 172.28, 172.10, 158.21, 139.37, 129.49, 129.41, 128.86, 60.07, 58.20, 57.47, 55.52, 41.75, 38.63, 36.41, 36.02, 28.88, 28.31, 26.64, 24.75, 21.18, 18.90, 11.06.

for $[M + H]^+$ 469.25, found 469.00. 1H NMR (300 MHz, CD_3OD) δ : 7.73 (d, $J = 7.5$ Hz, 2H), 7.58 (d, $J = 7.0$ Hz, 2H), 7.41–7.21 (m, 9H), 5.79–5.63 (m, 1H), 5.17 (s, 1H), 4.97–4.83 (m, 2H), 4.35 (d, $J = 6.7$ Hz, 2H), 4.18 (t, $J = 6.7$ Hz, 1H), 3.25–3.06 (m, 2H), 2.01–1.89 (m, 2H), 1.51–1.13 (m, 6H). ^{13}C NMR (75 MHz, CD_3OD) δ : 171.72, 157.16, 144.60, 144.51, 142.06, 139.40, 129.49, 128.96, 128.45, 127.83, 127.77, 125.78, 120.63, 114.88, 67.82, 59.48, 47.87, 40.29, 34.32, 29.66, 29.20, 26.91.

(*R*)-(9*H*-Fluoren-9-yl)methyl (2-(allyl(methyl)amino)-2-oxo-1-phenylethyl)carbamate (**32e**). Compound **32e** was prepared according to the procedure used for **32b** starting from **23c** and **31e**. The product was purified over flash chromatography using hexanes/EtOAc (1:1). White solid (84% yield). MS (ESI): m/z calcd for $[M + H]^+$ 427.20, found 427.08. 1H NMR (300 MHz, CD_3OD , rotamers) δ : 7.85–7.70 (m, 2H), 7.62–7.47 (m, 2H), 7.46–7.16 (m, 9H), 5.76–5.41 (m, 2H), 5.13–4.88 (m, 2H), 4.36–3.65 (m, 5H), 2.88 (s, 1.3H), 2.84 (s, 1.5H), 2.76 (s, 0.2H). ^{13}C NMR (75 MHz, CD_3OD , rotamers) δ : 172.32, 172.10, 158.01, 145.46, 145.29, 142.68, 138.58, 138.07, 133.55, 133.46, 130.24, 129.73, 129.41, 129.31, 128.93, 128.33, 126.46, 126.42, 121.07, 118.31, 117.84, 68.31, 57.61, 57.52, 52.99, 51.75, 48.50, 35.35, 34.36.

(*R*)-(9*H*-Fluoren-9-yl)methyl(2-(allyl(methyl)amino)-1-(4-fluorophenyl)-2-oxoethyl)carbamate (**32f**). Intermediate **32f** was prepared according to the procedure used for **32b** starting from **23a** and **31e**. The product was purified over flash chromatography using hexane/ethyl acetate (3:1). White solid (75% yield). MS (ESI): m/z calcd for $[M + H]^+$ 445.19, found 444.96. 1H NMR (300 MHz, CD_3OD , rotamers) δ : 7.88–7.72 (m, 2H), 7.65–7.50 (m, 2H), 7.47–7.19 (m, 6H), 7.14–6.78 (m, 2H), 5.80–5.51 (m, 2H), 5.17–5.03 (m, 2H), 4.42–4.19 (m, 3H), 4.11–3.88 (m, 2H), 2.90 (s, 1.2H), 2.87 (s, 1.5H), 2.77 (s, 0.3H). ^{13}C NMR (75 MHz, CD_3OD , rotamers) δ : 172.25, 172.00, 165.91, 162.64, 158.03, 157.98, 145.48, 145.31, 142.74, 134.73, 134.69, 134.21, 134.16, 133.54, 133.49, 131.54, 131.44, 131.35, 128.96, 128.34, 128.32, 126.43, 126.41, 121.09, 118.25, 117.90, 117.06, 116.77, 68.29, 56.80, 56.68, 53.03, 51.80, 48.56, 35.37, 34.44.

(*R*)-(9*H*-Fluoren-9-yl)methyl(2-(allyl(methyl)amino)-1-(4-chlorophenyl)-2-oxoethyl)carbamate (**32g**). Intermediate **32g** was prepared according to the procedure used for **32b** starting from **23b** and **31e**. The product was purified over flash chromatography using hexane/ethyl acetate (3:1). White solid (75% yield). MS (ESI): m/z calcd for $[M + H]^+$ 461.16, found 461.19. 1H NMR (300 MHz, CD_3OD , rotamers) δ : 7.88–7.72 (m, 2H), 7.65–7.50 (m, 2H), 7.47–7.20 (m, 6H), 7.14–7.04 (m, 2H), 5.78–5.47 (m, 2H), 5.15–5.01 (m, 2H), 4.38–4.25 (m, 2H), 4.23–4.13 (m, 1H), 4.08–3.85 (m, 2H), 2.90 (s, 1.2H), 2.87 (s, 1.5H), 2.77 (s, 0.3H). ^{13}C NMR (75 MHz, CD_3OD , rotamers) δ : 171.86, 171.59, 157.87, 145.39, 145.21, 142.65, 137.45, 136.95, 135.51, 133.45, 133.40, 131.00, 130.93, 130.24, 128.92, 128.30, 126.37, 121.07, 118.28, 117.95, 68.23, 56.74, 56.59, 52.98, 51.74, 48.48, 35.36, 34.44.

(9*H*-Fluoren-9-yl)methyl ((*S*)-1-(((*R*)-2-(Allylamino)-2-oxo-1-phenylethyl)amino)-1-oxobutan-2-yl)carbamate (**33a**). Intermediate **32a** (1.65 mmol, 0.68 g) was treated with diethylamine (33 mmol, 3.5 mL) in 100 mL of CH_3CN at 40 °C for 4 h followed by removal of the solvent and diethylamine in vacuo. The resulting crude was further dried under vacuum then taken into CH_2Cl_2 and mixed with Fmoc-2-Abu-OH (2.5 mmol, 0.81 g), EDCI (2.5 mmol, 0.48 g), HOAt (2.5 mmol, 0.34 g), and DIPEA (2.5 mmol, 0.44 mL) at room temperature for 4 h. The reaction mixture was quenched with H_2O and extracted to CH_2Cl_2 . The organic layer together with a white precipitate was collected and concentrated in vacuo. The remaining white solid was washed from CH_2Cl_2 yielding 0.57 g of intermediate **33a** as white powder (70% yield). HRMS (ESI): m/z calcd for $C_{30}H_{32}N_3O_4$ $[M + H]^+$ 498.2387, found 498.2392. 1H NMR (300 MHz, CD_3SO) δ : 8.56 (d, $J = 8.0$ Hz, 1H), 8.44 (t, $J = 5.5$ Hz, 1H), 7.89 (d, $J = 7.5$ Hz, 2H), 7.76–7.70 (m, 2H), 7.55 (d, $J = 8.1$ Hz, 1H), 7.45–7.38 (m, 4H), 7.36–7.22 (m, 4H), 5.80–5.67 (m, 1H), 5.48 (d, $J = 8.0$ Hz, 1H), 5.05–4.93 (m, 2H), 4.30–4.03 (m, 4H), 3.73–3.64 (m, 2H), 1.69–1.43 (m, 2H), 0.81 (t, $J = 7.3$ Hz, 3H). ^{13}C NMR (75 MHz, CD_3SO) δ : 171.52, 169.41, 156.07, 143.86, 143.75, 140.68, 138.99, 134.70,

128.22, 127.61, 127.45, 127.07, 126.88, 125.25, 120.07, 115.14, 65.67, 56.02, 55.91, 46.65, 40.81, 25.17, 10.35.

(9*H*-Fluoren-9-yl)methyl ((*S*)-1-(((*R*)-2-(Allyl(methyl)amino)-2-oxo-1-phenylethyl)amino)-1-oxobutan-2-yl)carbamate (**33e**). Compound **33e** was prepared according to Method A starting from **32e** (0.7 g 1.64 mmol). Fmoc-2-Abu-OH used as the amino acid. The compound was purified over flash chromatography using hexanes/EtOAc (1:1) affording 0.68 g of intermediate **33e** as white solid (81% yield). MS (ESI): m/z calcd for $[M + H]^+$ 512.25, found 512.58. 1H NMR (300 MHz, CD_3OD , 2-rotamers) δ : 7.78 (d, $J = 7.5$ Hz, 2H), 7.64 (d, $J = 7.3$ Hz, 2H), 7.42–7.24 (m, 9H), 5.85 (s, 0.55H), 5.83 (s, 0.45H), 5.77–5.42 (m, 1H), 5.14–4.97 (m, 2H), 4.39–4.24 (m, 2H), 4.22–4.00 (m, 3H), 3.96–3.82 (m, 1H), 2.89 (s, 3H), 1.84–1.51 (m, 2H), 0.86 (t, $J = 7.4$ Hz, 3H). ^{13}C NMR (75 MHz, CD_3OD , 2-rotamers) δ : 174.01, 173.94, 171.69, 171.46, 158.59, 145.56, 145.35, 142.77, 138.50, 138.01, 133.54, 133.49, 130.25, 129.77, 129.37, 129.29, 128.96, 128.39, 128.35, 126.43, 126.36, 121.11, 118.37, 117.89, 68.21, 58.03, 55.84, 55.71, 53.07, 51.74, 35.37, 34.31, 26.73, 10.76.

(9*H*-Fluoren-9-yl)methyl ((6*S*,9*S*,12*R*)-9-Ethyl-1-imino-7,10,13-trioxo-1-(2,2,4,6,7-pentamethyl-2,3-dihydrobenzofuran-5-sulfonamido)-12-phenyl-2,8,11,14-tetraazaheptadec-16-en-6-yl)carbamate (**34a**). A method applied for **33a** was used to make **34a** starting from **33a**. White solid (83% yield). HRMS (ESI): m/z calcd for $C_{49}H_{60}N_9O_8S$ $[M + H]^+$ 906.4219, found 906.4222. 1H NMR (300 MHz, CD_3SO) δ : 8.59 (d, $J = 8.1$ Hz, 1H), 8.45 (t, $J = 5.7$ Hz, 1H), 7.96 (d, $J = 7.6$ Hz, 1H), 7.89 (d, $J = 7.4$ Hz, 2H), 7.75–7.67 (m, 2H), 7.53 (d, $J = 8.2$ Hz, 1H), 7.44–7.37 (m, 4H), 7.35–7.22 (m, 5H), 5.80–5.66 (m, 1H), 5.48 (d, $J = 8.1$ Hz, 1H), 5.04–4.94 (m, 2H), 4.39–4.17 (m, 4H), 4.08–3.96 (m, 1H), 3.72–3.64 (m, 2H), 3.07–2.98 (m, 2H), 2.93 (s, 2H), 2.49 (s, 3H), 2.43 (s, 3H), 1.99 (s, 3H), 1.72–1.35 (m, 12H), 0.77 (t, $J = 7.3$ Hz, 3H). ^{13}C NMR (75 MHz, CD_3SO): δ 171.77, 170.96, 169.40, 157.44, 156.05, 155.91, 143.85, 143.72, 140.69, 138.93, 137.26, 134.70, 134.20, 131.43, 128.22, 127.61, 127.47, 127.06, 126.93, 125.26, 124.30, 120.06, 116.25, 115.13, 86.25, 65.62, 56.03, 53.68, 46.67, 42.45, 40.84, 28.25, 25.33, 18.92, 17.58, 12.23, 10.02.

(9*H*-Fluoren-9-yl)methyl ((6*S*,9*S*,12*R*)-9-Ethyl-1-imino-14-methyl-7,10,13-trioxo-1-(2,2,4,6,7-pentamethyl-2,3-dihydrobenzofuran-5-sulfonamido)-12-phenyl-2,8,11,14-tetraazaheptadec-16-en-6-yl)carbamate (**34e**). Compound **34e** was prepared according to Method A starting from **33e** (0.66 g 1.29 mmol). Fmoc-Arg(Pbf)-OH used as the amino acid. The compound was purified over flash chromatography using hexanes/EtOAc (1:1) affording 1.0 g (1.09 mmol) of intermediate **34e** as white solid (84% yield). MS (ESI): m/z calcd for $[M + H]^+$ 920.44, found 920.25. 1H NMR (300 MHz, CD_3OD , 2-rotamers) δ : 7.79 (d, $J = 7.5$ Hz, 2H), 7.66 (t, $J = 7.2$ Hz, 2H), 7.42–7.26 (m, 9H), 5.81 (s, 0.5H), 5.79 (s, 0.5H), 5.74–5.58 (m, 1H), 5.11–4.97 (m, 2H), 4.40–4.29 (m, 3H), 4.21 (t, $J = 6.5$ Hz, 1H), 4.11–3.98 (m, 2H), 3.91–3.80 (m, 1H), 3.19–3.10 (m, 2H), 2.96 (s, 2H), 2.86 (s, 3H), 2.58 (s, 3H), 2.51 (s, 3H), 2.06 (s, 3H), 1.87–1.46 (m, 6H), 1.42 (s, 6H), 0.85 (t, $J = 7.1$ Hz, 3H). ^{13}C NMR (75 MHz, CD_3OD , rotamers) δ : 174.86, 173.27, 171.71, 171.54, 160.07, 158.70, 158.33, 145.65, 145.33, 142.80, 139.62, 137.70, 134.63, 133.73, 133.55, 133.46, 130.28, 129.83, 129.52, 129.42, 129.00, 128.38, 126.44, 126.23, 121.13, 118.65, 118.42, 117.82, 87.85, 68.21, 56.42, 56.07, 56.00, 53.08, 51.78, 44.17, 41.77, 35.41, 34.37, 30.63, 28.89, 26.94, 26.41, 19.79, 18.60, 12.71, 10.76.

(9*H*-Fluoren-9-yl)methyl ((8*S*,11*S*,14*R*,*E*)-11-Ethyl-9,12,15-trioxo-3-(2,2,4,6,7-pentamethyl-2,3-dihydrobenzofuran-5-sulfonamido)-14-phenyl-2,4,10,13,16-pentaazanadeca-2,18-dien-8-yl)carbamate (**34h**). A method similar that applied for **33a** was used for the synthesis of **34h** starting from **33a** (0.5 g, 1 mmol). Fmoc-Arg(Me) (Pbf)-OH was used as the amino acid. Intermediate **34h** (0.36 g) was obtained as white solid (65% yield) and used for the next step without further purification. MS (ESI): m/z calcd for $[M + H]^+$ 920.44, found 920.25.

(9*H*-Fluoren-9-yl)methyl ((6*R*,9*S*,12*S*,15*R*)-9-Ethyl-15-methyl-5,8,11,14-tetraoxo-12-(3-(3-(2,2,4,6,7-pentamethyl-2,3-dihydrobenzofuran-5-yl)sulfonyl)guanidino)propyl)-6-phenyl-4,7,10,13-tetraazaoctadeca-1,17-dien-15-yl)carbamate (**35a**). Intermediate **34a** (1.18 g, 1.3 mmol) was treated with diethylamine (26 mmol, 2.7 mL)

in 50 mL of CH₃CN at 40 °C for 2 h followed by removal of the solvent and diethylamine in vacuo. The resulting crude was taken into CH₂Cl₂ and mixed with **21** (2 mmol, 0.7 g), EDCI (2 mmol, 0.38 g), HOAt (2 mmol, 0.27 g), and DIPEA (2 mmol, 0.35 mL) at room temperature for 4 h. The reaction mixture was quenched with H₂O and extracted to CH₂Cl₂. The organic layers were collected and dried over anhydrous sodium sulfate, filtered, evaporated, and purified over flash chromatography using EtAc/MeOH (50:0.7) yielding 0.8 g of intermediate **35a** as white solid (60% yield). HRMS (ESI): *m/z* calcd for C₅₅H₆₉N₈O₉S [M + H]⁺ 1017.4903, found 1017.4899. ¹H NMR (300 MHz, MeOD) δ: 7.79 (d, *J* = 7.4 Hz, 2H), 7.65 (d, *J* = 7.4 Hz, 2H), 7.43–7.25 (m, 9H), 5.77–5.60 (m, 2H), 5.40 (s, 1H), 5.11–4.92 (m, 4H), 4.52–4.43 (m, 1H), 4.36–4.15 (m, 4H), 3.84–3.64 (m, 2H), 3.17–3.09 (m, 2H), 2.95 (s, 2H), 2.67–2.39 (m, 8H), 2.05 (s, 3H), 1.96–1.45 (m, 6H), 1.41 (s, 6H), 1.34 (s, 3H), 0.89 (t, *J* = 7.2 Hz, 3H). ¹³C NMR (75 MHz, CD₃OD): δ 171.77, 170.96, 169.40, 157.44, 156.05, 155.91, 143.85, 143.72, 140.69, 138.93, 137.26, 134.70, 134.20, 131.43, 128.22, 127.61, 127.47, 127.06, 126.93, 125.26, 124.30, 120.06, 116.25, 115.13, 86.25, 65.62, 56.03, 53.68, 46.67, 42.45, 40.84, 28.25, 25.33, 18.92, 17.58, 12.23, 10.02.

(9*H*-Fluoren-9-yl)methyl ((6*R*,9*S*,12*S*,15*R*)-9-Ethyl-4,15-dimethyl-5,8,11,14-tetraoxo-12-(3-(3-((2,2,4,6,7-pentamethyl-2,3-dihydrobenzofuran-5-yl)sulfonyl)guanidino)propyl)-6-phenyl-4,7,10,13-tetraazaoctadeca-1,17-dien-15-yl)carbamate (**35e**). Compound **35e** was prepared according to Method A starting from **34e** (0.9 g 1.0 mmol). Intermediate **21** was used as the amino acid. The compound was purified over flash chromatography using hexanes/EtOAc (1:1) affording 0.83 g (0.8 mmol) intermediate **35e** as white solid (80% yield). MS (ESI): *m/z* calcd for [M + H]⁺ 1031.51, found 1031.75. ¹H NMR (300 MHz, CD₃OD, rotamers) δ: 7.79 (d, *J* = 7.4 Hz, 2H), 7.68–7.62 (m, 2H), 7.44–7.24 (m, 9H), 5.78–5.76 (m, 1H), 5.74–5.43 (m, 2H), 5.12–4.96 (m, 4H), 4.59–4.48 (m, 1H), 4.35–4.15 (m, 4H), 4.07–3.77 (m, 2H), 3.17–3.08 (m, 2H), 2.95 (s, 2H), 2.87 (s, 0.2H), 2.85 (s, 1.6H), 2.83 (s, 1.2H), 2.64–2.36 (m, 8H), 2.05 (s, 3H), 1.94–1.45 (m, 6H), 1.42 (s, 6H), 1.33 (s, 3H), 0.87 (t, *J* = 7.2 Hz, 3H). ¹³C NMR (75 MHz, CD₃OD) δ: 176.90, 174.37, 173.49, 171.57, 171.37, 160.05, 158.29, 157.88, 145.51, 145.44, 142.87, 142.85, 139.60, 137.69, 134.65, 134.06, 133.71, 133.62, 130.19, 129.76, 129.56, 129.46, 129.01, 128.39, 126.46, 126.34, 126.21, 121.15, 119.98, 118.63, 118.37, 117.79, 87.84, 67.99, 60.45, 56.82, 56.09, 55.89, 54.88, 53.09, 51.75, 44.17, 41.80, 35.37, 34.33, 29.85, 28.90, 27.04, 26.34, 23.51, 19.77, 18.58, 12.71, 11.13.

(9*H*-Fluoren-9-yl)methyl ((6*R*,9*S*,12*S*,15*R*)-9-Ethyl-6-(4-fluorophenyl)-4,15-dimethyl-5,8,11,14-tetraoxo-12-(3-(3-((2,2,4,6,7-pentamethyl-2,3-dihydrobenzofuran-5-yl)sulfonyl)guanidino)propyl)-4,7,10,13-tetraazaoctadeca-1,17-dien-15-yl)carbamate (**35f**). Intermediate **35f** was prepared according to Method A starting from **32f**. Intermediate **28** was used as the peptide carboxylic acid. The crude was purified over flash chromatography using ethyl acetate. White solid (45% yield). MS (ESI): *m/z* calcd for [M + H]⁺ 1049.26, found 1049.66. ¹H NMR (300 MHz, CD₃OD, 2-rotamers) δ: 7.80 (d, *J* = 7.5 Hz, 2H), 7.71–7.61 (m, 2H), 7.46–7.26 (m, 6H), 7.10–6.99 (m, 2H), 5.78 (s, 1H), 5.75–5.49 (m, 2H), 5.11–4.96 (m, 4H), 4.61–4.49 (m, 1H), 4.37–4.26 (m, 1H), 4.26–4.13 (m, 3H), 4.05–3.75 (m, 2H), 3.17–3.10 (m, 2H), 2.96 (s, 2H), 2.87 (s, 1.6H), 2.83 (s, 1.4H), 2.63–2.35 (m, 8H), 2.06 (s, 3H), 1.93–1.46 (m, 6H), 1.42 (s, 6H), 1.32 (s, 3H), 0.87 (t, *J* = 7.3 Hz, 3H). ¹³C NMR (75 MHz, CD₃OD, rotamers) δ: 177.06, 176.97, 174.47, 173.57, 173.51, 171.40, 171.17, 165.83, 162.55, 160.02, 158.25, 157.92, 145.46, 145.40, 142.83, 142.81, 139.56, 134.63, 134.03, 133.68, 133.62, 133.57, 131.69, 131.58, 131.49, 129.01, 128.37, 126.43, 126.31, 126.19, 121.16, 120.01, 118.61, 118.30, 117.86, 117.00, 116.94, 116.71, 116.65, 87.81, 68.01, 60.38, 56.85, 55.26, 55.00, 53.06, 51.75, 44.14, 41.68, 35.36, 34.40, 29.73, 28.89, 27.15, 26.29, 26.23, 23.58, 19.80, 18.60, 12.72, 11.21.

(9*H*-Fluoren-9-yl)methyl ((6*R*,9*S*,12*S*,15*R*)-6-(4-Chlorophenyl)-9-ethyl-4,15-dimethyl-5,8,11,14-tetraoxo-12-(3-(3-((2,2,4,6,7-pentamethyl-2,3-dihydrobenzofuran-5-yl)sulfonyl)guanidino)propyl)-4,7,10,13-tetraazaoctadeca-1,17-dien-15-yl)carbamate (**35g**). Intermediate **35g** was prepared according to Method A starting from **32g**. Intermediate **28** was used as the peptide carboxylic acid. The product was purified over flash chromatography using ethyl acetate.

White solid (44% yield). MS (ESI): *m/z* calcd for [M + H]⁺ 1065.47, found 1065.08. ¹H NMR (300 MHz, CD₃OD, 2-rotamers) δ: 7.80 (d, *J* = 7.5 Hz, 2H), 7.69–7.62 (m, 2H), 7.43–7.25 (m, 8H), 5.78 (s, 1H), 5.73–5.50 (m, 2H), 5.12–4.97 (m, 4H), 4.60–4.51 (m, 1H), 4.35–4.27 (m, 1H), 4.25–4.14 (m, 3H), 4.04–3.78 (m, 2H), 3.19–3.09 (m, 2H), 2.96 (s, 2H), 2.90–2.81 (m, 3H), 2.62–2.36 (m, 8H), 2.06 (s, 3H), 1.94–1.46 (m, 6H), 1.42 (s, 6H), 1.32 (s, 3H), 0.88 (t, *J* = 7.3 Hz, 3H). ¹³C NMR (75 MHz, CD₃OD, rotamers) δ: 177.03, 174.50, 173.64, 173.59, 171.18, 170.94, 160.04, 158.27, 157.96, 145.47, 145.42, 142.84, 139.58, 137.09, 136.55, 135.55, 135.46, 134.63, 134.06, 134.04, 133.69, 133.65, 133.57, 131.24, 131.16, 130.22, 130.15, 129.02, 128.38, 126.45, 126.31, 126.20, 121.17, 120.03, 118.62, 118.32, 117.92, 87.82, 68.02, 60.38, 56.91, 55.31, 55.03, 53.09, 51.78, 44.15, 41.66, 35.38, 34.43, 29.71, 28.90, 27.16, 26.28, 26.22, 23.58, 19.80, 18.61, 12.73, 11.24.

(9*H*-Fluoren-9-yl)methyl ((6*R*,9*S*,12*S*,15*R*)-9-Ethyl-15-methyl-12-(3-((E)-2-methyl-3-((2,2,4,6,7-pentamethyl-2,3-dihydrobenzofuran-5-yl)sulfonyl)guanidino)propyl)-5,8,11,14-tetraoxo-6-phenyl-4,7,10,13-tetraazaoctadeca-1,17-dien-15-yl)carbamate (**35h**). Intermediate **35h** was prepared according to Method A starting from **34h** (0.33 g 0.35 mmol). Intermediate **21** was used as the amino acid. The compound was purified over flash chromatography using EtOAc/MeOH (10:0.1) affording 0.29 g (0.28 mmol) of intermediate **35h** as white solid (85% yield). MS (ESI): *m/z* calcd for [M + H]⁺ 1031.51, found 1031.08. ¹H NMR (300 MHz, CD₃OD) δ: 7.79 (d, *J* = 7.4 Hz, 2H), 7.65 (d, *J* = 7.4 Hz, 2H), 7.42–7.25 (m, 9H), 5.78–5.60 (m, 2H), 5.40 (s, 1H), 5.12–4.91 (m, 4H), 4.52–4.43 (m, 1H), 4.36–4.15 (m, 4H), 3.84–3.64 (m, 2H), 3.20–3.09 (m, 2H), 2.95 (s, 2H), 2.73 (s, 3H), 2.67–2.40 (m, 8H), 2.05 (s, 3H), 1.95–1.46 (m, 6H), 1.42 (s, 6H), 1.35 (s, 3H), 0.89 (t, *J* = 7.4 Hz, 3H). ¹³C NMR (75 MHz, CD₃OD) δ: 174.56, 174.06, 172.31, 160.00, 158.02, 157.57, 145.42, 145.38, 142.85, 139.46, 138.78, 135.33, 134.83, 134.02, 133.58, 129.94, 129.51, 129.08, 129.04, 128.39, 126.40, 126.35, 126.22, 121.18, 120.04, 118.65, 116.32, 87.83, 68.08, 60.42, 59.35, 57.02, 44.16, 42.91, 42.10, 41.87, 28.91, 28.70, 25.97, 23.58, 19.86, 18.66, 12.72, 11.16.

(*R*)-*N*-((6*S*,9*S*,12*R*)-9-Ethyl-1-imino-7,10,13-trioxo-1-(2,2,4,6,7-pentamethyl-2,3-dihydrobenzofuran-5-sulfonamido)-12-phenyl-2,8,11,14-tetraazaheptadec-16-en-6-yl)-2-isobutyramido-2-methylpent-4-enamide (**36a**). Intermediate **35a** (0.43 mmol, 0.44 g) was dissolved in 50 mL of CH₃CN and treated with 20 equiv of diethylamine (8.6 mmol, 0.63 mL) at room temperature for 2 h. The solvent and diethylamine were removed in vacuo, and the resulting crude was mixed with isobutyryl chloride (1.9 mmol, 0.2 mL) and DIPEA (1.9 mmol, 0.33 mL) in CH₂Cl₂ at room temperature for 2 h. The reaction mixture was evaporated, and the remaining crude was purified over flash chromatography using EtAc/MeOH (50:0.7) yielding 0.23 g of intermediate (**36a**) as white solid (62% yield). HRMS (ESI): *m/z* calcd for C₄₄H₆₅N₈O₈S [M + H]⁺ 865.4641, found 865.4642. ¹H NMR (300 MHz, CD₃OD) δ: 7.45–7.28 (m, 5H), 5.84–5.64 (m, 2H), 5.42 (s, 1H), 5.14–4.99 (m, 4H), 4.26–4.19 (m, 2H), 3.89–3.69 (m, 2H), 3.15 (t, *J* = 6.7 Hz, 2H), 2.99 (s, 2H), 2.74–2.65 (m, 1H), 2.60–2.40 (m, 8H), 2.07 (s, 3H), 1.98–1.48 (m, 6H), 1.45 (s, 6H), 1.37 (s, 3H), 1.13–1.06 (m, 6H), 0.92 (t, *J* = 7.4 Hz, 3H). ¹³C NMR (75 MHz, CD₃OD): δ 180.33, 176.96, 174.56, 174.22, 172.49, 160.08, 158.33, 139.58, 138.59, 135.36, 134.61, 134.16, 133.72, 129.93, 129.55, 129.21, 126.22, 119.95, 118.64, 116.31, 87.87, 59.99, 59.54, 56.93, 55.03, 44.19, 42.92, 41.24, 36.15, 30.01, 28.91, 25.96, 23.42, 20.43, 20.03, 19.84, 19.75, 18.57, 12.69, 11.25.

(*R*)-*N*-((6*S*,9*S*,12*R*)-9-Ethyl-1-imino-7,10,13-trioxo-1-(2,2,4,6,7-pentamethyl-2,3-dihydrobenzofuran-5-sulfonamido)-12-phenyl-2,8,11,14-tetraazaheptadec-17-en-6-yl)-2-isobutyramido-2-methylpent-4-enamide (**36b**). Intermediate **36b** was prepared according to Method A starting from **32b**. Intermediate **26** was used as the peptide carboxylic acid. The crude was purified over flash chromatography using EtOAc/MeOH (30:1). White solid (72% yield). MS (ESI): *m/z* calcd for [M + H]⁺ 879.48, found 879.42. ¹H NMR (300 MHz, CD₃OD) δ: 7.44–7.23 (m, 5H), 5.80–5.63 (m, 2H), 5.40 (s, 1H), 5.15–4.91 (m, 4H), 4.27–4.17 (m, 2H), 3.28–3.09 (m, 4H), 2.99 (s, 2H), 2.76–2.65 (m, 1H), 2.61–2.40 (m, 8H), 2.21 (q, *J* = 6.9 Hz, 2H), 2.07 (s, 3H), 1.97–1.48 (m, 6H), 1.44 (s, 6H), 1.37 (s, 3H), 1.15–1.04 (m, 6H), 0.92 (t, *J* = 7.4 Hz, 3H). ¹³C NMR (75 MHz, CD₃OD)

δ : 180.29, 176.98, 174.53, 174.16, 172.47, 160.03, 158.24, 139.55, 138.53, 136.56, 134.55, 134.14, 133.67, 129.86, 129.48, 129.21, 126.18, 119.99, 118.60, 117.44, 87.83, 59.89, 59.47, 56.90, 55.09, 44.16, 41.66, 41.17, 40.27, 36.08, 34.86, 29.88, 28.94, 27.12, 25.95, 23.42, 20.51, 19.83, 18.64, 12.76, 11.32.

(9*H*-Fluoren-9-yl)methyl ((4*R*,7*S*,10*S*,13*R*)-10-Ethyl-4-methyl-5,8,11,14-tetraoxo-7-(3-(3-((2,2,4,6,7-pentamethyl-2,3-dihydrobenzofuran-5-yl)sulfonyl)guanidino)propyl)-13-phenyl-6,9,12,15-tetrazaicoso-1,19-dien-4-yl)carbamate (**36c**). Intermediate **36c** was prepared according to Method A starting from **32c**. Intermediate **26** was used as the peptide carboxylic acid. The crude was purified over flash chromatography using EtOAc/MeOH (25:4). White solid (80% yield). MS (ESI): m/z calcd for $[M + H]^+$ 893.50, found 893.62. 1H NMR (300 MHz, CD_3OD) δ : 7.43–7.26 (m, 5H), 5.84–5.64 (m, 2H), 5.38 (s, 1H), 5.14–4.91 (m, 4H), 4.26–4.18 (m, 2H), 3.28–3.06 (m, 4H), 2.99 (s, 2H), 2.75–2.64 (m, 1H), 2.61–2.41 (m, 8H), 2.08 (s, 3H), 2.05–1.48 (m, 10H), 1.45 (s, 6H), 1.37 (s, 3H), 1.14–1.06 (m, 6H), 0.92 (t, $J = 7.4$ Hz, 3H). ^{13}C NMR (75 MHz, CD_3OD) δ : 180.31, 176.94, 174.56, 174.18, 172.50, 160.08, 158.33, 139.59, 139.24, 138.69, 134.61, 134.14, 133.72, 129.91, 129.51, 129.18, 126.22, 119.96, 118.64, 115.72, 87.87, 59.99, 59.51, 56.96, 50.55, 44.20, 41.28, 40.34, 36.15, 32.24, 30.00, 29.92, 28.91, 27.04, 25.97, 23.40, 20.45, 19.85, 19.76, 18.58, 12.69, 11.26.

(*R*)-*N*-((6*S*,9*S*,12*R*)-9-Ethyl-1-imino-7,10,13-trioxo-1-(2,2,4,6,7-pentamethyl-2,3-dihydrobenzofuran-5-sulfonamido)-12-phenyl-2,8,11,14-tetrazaheptacos-20-en-6-yl)-2-isobutyramido-2-methylpent-4-enamide (**36d**). Intermediate **36d** was prepared according to Method A starting from **32d**. Intermediate **26** was used as the peptide carboxylic acid. The crude was purified over flash chromatography using EtOAc/MeOH (40:1) to afford **36d** as white solid (71% yield). MS (ESI): m/z calcd for $[M + H]^+$ 921.53, found 921.42. 1H NMR (300 MHz, CD_3OD) δ : 7.43–7.28 (m, 5H), 5.83–5.64 (m, 2H), 5.39 (s, 1H), 5.14–4.90 (m, 4H), 4.25–4.19 (m, 2H), 3.26–3.07 (m, 4H), 2.99 (s, 2H), 2.74–2.65 (m, 1H), 2.58–2.41 (m, 8H), 2.07 (s, 3H), 2.04–1.46 (m, 10H), 1.45 (s, 6H), 1.37 (s, 3H), 1.35–1.21 (m, 4H), 1.13–1.08 (m, 6H), 0.92 (t, $J = 7.4$ Hz, 3H). ^{13}C NMR (75 MHz, CD_3OD) δ : 180.32, 177.00, 174.56, 174.15, 172.45, 160.06, 158.29, 140.09, 139.57, 138.66, 134.57, 134.16, 133.70, 129.89, 129.49, 129.18, 126.20, 119.98, 118.62, 115.10, 87.85, 59.93, 59.50, 56.90, 50.10, 44.18, 41.70, 41.22, 40.73, 36.12, 34.97, 30.46, 29.94, 28.92, 27.54, 27.08, 25.97, 23.40, 20.49, 19.83, 19.79, 18.61, 12.72, 11.30.

(*R*)-*N*-((6*S*,9*S*,12*R*)-9-Ethyl-1-imino-14-methyl-7,10,13-trioxo-1-(2,2,4,6,7-pentamethyl-2,3-dihydrobenzofuran-5-sulfonamido)-12-phenyl-2,8,11,14-tetrazaheptadec-16-en-6-yl)-2-isobutyramido-2-methylpent-4-enamide (**36e**). Intermediate **36e** was prepared starting from **35e** according to the procedure used for **36a**. The reaction mixture was concentrated under vacuum, and the remaining crude was purified over flash chromatography using EtAc/MeOH (20:1) yielding 0.19 g intermediate **36e** as white solid (45% yield). MS (ESI): m/z calcd for $[M + H]^+$ 879.48, found 879.78. 1H NMR (300 MHz, CD_3OD , 2-rotamers) δ : 7.44–7.27 (m, 5H), 5.80 (s, 1H), 5.76–5.47 (m, 2H), 5.16–4.99 (m, 4H), 4.31–4.18 (m, 2H), 4.07–3.81 (m, 2H), 3.19–3.10 (m, 2H), 3.00 (s, 2H), 2.90 (s, 1.6H), 2.87 (s, 1.4H), 2.69–2.38 (m, 9H), 2.08 (s, 3H), 1.92–1.47 (m, 6H), 1.45 (s, 6H), 1.36 (s, 3H), 1.09 (d, $J = 6.8$ Hz, 6H), 0.90 (t, $J = 7.4$ Hz, 3H). ^{13}C NMR (75 MHz, CD_3OD , rotamers) δ : 180.00, 176.66, 176.55, 174.35, 174.29, 173.66, 171.65, 171.46, 160.06, 158.31, 139.59, 138.21, 137.63, 134.65, 134.19, 133.72, 133.64, 130.18, 130.14, 129.79, 129.70, 129.62, 129.52, 126.20, 119.87, 118.62, 118.39, 117.78, 87.86, 60.06, 56.84, 56.16, 55.93, 54.84, 54.73, 53.15, 51.81, 44.19, 41.76, 41.30, 36.15, 35.42, 34.37, 30.20, 28.91, 26.81, 26.36, 26.27, 23.36, 20.41, 20.38, 19.85, 19.77, 18.59, 12.70, 11.24.

(*R*)-*N*-((6*S*,9*S*,12*R*)-9-Ethyl-12-(4-fluorophenyl)-1-imino-14-methyl-7,10,13-trioxo-1-(2,2,4,6,7-pentamethyl-2,3-dihydrobenzofuran-5-sulfonamido)-2,8,11,14-tetrazaheptadec-16-en-6-yl)-2-isobutyramido-2-methylpent-4-enamide (**36f**). Intermediate **36f** was prepared starting from **35f** according to the procedure used for **36a**. The compound was purified over flash chromatography using ethyl acetate/MeOH (15:1). White solid (58% yield). MS (ESI): m/z calcd for $[M + H]^+$ 897.47, found 897.76. 1H NMR (300 MHz, CD_3OD , 2-rotamers) δ : 7.47–7.38 (m, 2H), 7.11–7.01 (m, 2H), 5.81

(s, 1H), 5.77–5.61 (m, 2H), 5.16–5.01 (m, 4H), 4.27–4.17 (m, 2H), 4.09–3.81 (m, 2H), 3.21–3.11 (m, 2H), 3.00 (s, 2H), 2.92 (s, 1.6H), 2.87 (s, 1.4H), 2.68–2.37 (m, 9H), 2.08 (s, 3H), 1.93–1.43 (m, 12H), 1.35 (s, 3H), 1.09 (d, $J = 6.8$ Hz, 6H), 0.90 (t, $J = 7.3$ Hz, 3H). ^{13}C NMR (75 MHz, CD_3OD , rotamers) δ : 180.05, 176.88, 176.73, 174.45, 174.37, 173.74, 171.50, 171.30, 165.89, 162.62, 160.06, 158.31, 139.57, 134.62, 134.23, 134.18, 133.83, 133.70, 133.62, 131.78, 131.68, 131.57, 126.20, 119.89, 118.62, 118.35, 117.85, 116.99, 116.89, 116.70, 116.60, 87.85, 59.98, 59.96, 56.96, 56.92, 55.35, 55.06, 53.16, 51.83, 44.18, 41.73, 41.10, 36.12, 35.41, 34.43, 30.04, 28.91, 26.94, 26.33, 26.22, 23.42, 20.48, 20.45, 19.82, 19.77, 18.59, 12.70, 11.35, 11.28.

(*R*)-*N*-((6*S*,9*S*,12*R*)-12-(4-Chlorophenyl)-9-ethyl-1-imino-14-methyl-7,10,13-trioxo-1-(2,2,4,6,7-pentamethyl-2,3-dihydrobenzofuran-5-sulfonamido)-2,8,11,14-tetrazaheptadec-16-en-6-yl)-2-isobutyramido-2-methylpent-4-enamide (**36g**). Intermediate **36g** was prepared starting from **35g** according to the procedure used for **36a**. The compound was purified over flash chromatography using ethyl acetate/MeOH (70:1). White solid (76% yield). MS (ESI): m/z calcd for $[M + H]^+$ 913.44, found 913.42. 1H NMR (300 MHz, CD_3OD , 2-rotamers) δ : 7.45–7.29 (m, 4H), 5.81 (s, 1H), 5.77–5.62 (m, 2H), 5.17–5.02 (m, 4H), 4.27–4.16 (m, 2H), 4.09–3.87 (m, 2H), 3.19–3.12 (m, 2H), 3.00 (s, 2H), 2.92 (s, 1.7H), 2.87 (s, 1.3H), 2.67–2.38 (m, 9H), 2.08 (s, 3H), 1.92–1.43 (m, 12H), 1.35 (m, 3H), 1.09 (d, $J = 6.9$ Hz, 6H), 0.91 (t, $J = 7.4$ Hz, 3H). ^{13}C NMR (75 MHz, CD_3OD , rotamers) δ : 180.05, 176.98, 176.79, 174.52, 174.43, 173.77, 171.25, 171.04, 160.03, 158.26, 139.54, 137.07, 136.47, 135.53, 135.40, 134.60, 134.20, 134.15, 133.82, 133.67, 133.57, 131.30, 131.22, 130.18, 130.08, 126.18, 119.94, 118.60, 118.40, 117.94, 87.83, 59.93, 57.00, 55.38, 55.23, 55.05, 53.17, 51.84, 44.17, 41.70, 41.04, 40.92, 36.08, 35.43, 34.46, 29.93, 29.86, 28.93, 27.00, 26.27, 26.14, 23.43, 20.52, 20.47, 19.80, 18.61, 12.74, 11.42, 11.34.

(*R*)-*N*-((8*S*,11*S*,14*R*,*E*)-11-Ethyl-9,12,15-trioxo-3-(2,2,4,6,7-pentamethyl-2,3-dihydrobenzofuran-5-sulfonamido)-14-phenyl-2,4,10,13,16-pentaazanonadeca-2,18-dien-8-yl)-2-isobutyramido-2-methylpent-4-enamide (**36h**). Intermediate **36h** was prepared starting from **35h** according to the procedure used for **36a**. The compound was purified over flash chromatography using EtOAc/MeOH (250:4). White solid (59% yield). MS (ESI): m/z calcd for $[M + H]^+$ 879.48, found 879.50. 1H NMR (300 MHz, CD_3OD) δ : 7.45–7.40 (m, 2H), 7.37–7.25 (m, 3H), 5.85–5.64 (m, 2H), 5.45 (s, 1H), 5.14–4.99 (m, 4H), 4.27–4.20 (m, 2H), 3.90–3.69 (m, 2H), 3.21–3.12 (m, 2H), 2.98 (s, 2H), 2.75 (s, 3H), 2.73–2.65 (m, 1H), 2.58 (s, 3H), 2.56–2.41 (m, 5H), 2.07 (s, 3H), 2.00–1.49 (m, 6H), 1.44 (s, 6H), 1.37 (s, 3H), 1.14–1.06 (m, 6H), 0.93 (t, $J = 7.4$ Hz, 3H). ^{13}C NMR (75 MHz, CD_3OD) δ : 180.28, 176.97, 174.49, 174.12, 172.41, 159.96, 157.51, 139.39, 138.53, 135.33, 134.83, 134.15, 133.52, 129.88, 129.49, 129.17, 126.17, 119.95, 118.60, 116.28, 87.81, 59.89, 59.50, 56.89, 55.01, 44.15, 42.86, 42.07, 41.14, 36.07, 29.88, 28.94, 28.72, 27.11, 25.93, 23.46, 20.49, 19.87, 19.82, 18.67, 12.74, 11.30.

(*R*)-*N*-((8*S*,11*S*,14*R*,*Z*)-11-ethyl-3-(methylamino)-9,12,15-trioxo-14-phenyl-2,4,10,13,16-pentaazanonadeca-2,18-dien-8-yl)-2-isobutyramido-2-methylpent-4-enamide (**36i**). Intermediate **36i** was prepared according to Method A starting from **32a**. Intermediate **30** was used as the peptide carboxylic acid. The crude was purified with preparative HPLC using the C18 reverse phase column (Waters, Sunfire Prep C₁₈ OBD, 5 μ m, 50 mm \times 100 mm). White solid (44% yield). MS (ESI): m/z calcd for $[M + H]^+$ 641.41, found 641.42. 1H NMR (300 MHz, CD_3OD) δ : 7.45–7.28 (m, 5H), 5.87–5.65 (m, 2H), 5.42 (s, 1H), 5.16–5.01 (m, 4H), 4.27–4.16 (m, 2H), 4.32 (dd, $J = 5.0, 7.6$ Hz, 1H), 4.25 (dd, $J = 5.7, 8.8$ Hz, 1H), 3.90–3.72 (m, 2H), 3.20 (t, $J = 7.0$ Hz, 2H), 2.83 (s, 6H), 2.74–2.64 (m, 1H), 2.60–2.41 (m, 2H), 1.99–1.57 (m, 6H), 1.39 (m, 3H), 1.15–1.07 (m, 6H), 0.93 (t, $J = 7.4$ Hz, 3H). ^{13}C NMR (75 MHz, CD_3OD) δ : 180.33, 176.81, 174.35, 174.13, 172.46, 157.45, 138.61, 135.35, 133.98, 129.94, 129.58, 129.15, 119.97, 116.33, 60.05, 59.51, 56.86, 54.42, 42.92, 42.13, 41.69, 36.07, 30.19, 28.50, 26.17, 26.04, 23.19, 20.38, 19.79, 11.12.

(*R*)-2-(((9*H*-fluoren-9-yl)methoxy)carbonyl)amino-4-(dibenzylamino)-2-methylbutanoic Acid CF_3COOH Salt (**40**). (*R*)-2-Fmoc-NH-2-methylpent-4-enoic acid (1 mmol, 350 mg) was dissolved in THF/H₂O (2.6 mL/1 mL) in a flask. The hood lights were turned off, and the flask was covered with aluminum foil. Osmium tetroxide (0.05

mmol in 0.32 mL of H₂O) was added to the flask. After 5 min, NaIO₄ (2.5 mmol, 535 mg) was added in small portions over a 15 min period. The reaction was kept at room temperature for 4 h before it was filtered, and the THF was evaporated off. The residue was dissolved in EtOAc, and saturated NH₄Cl aqueous solution was added. The aqueous phase was extracted with EtOAc (2 × 30 mL) and the organic phase was combined, washed with brine, and dried over anhydrous Na₂SO₄. The solution was concentrated in vacuo, and the crude product was dissolved in 1,2-dichloroethane (3 mL) in a flask. Then dibenzylamine (1.5 mmol, 0.29 mL) and sodium triacetoxyborohydride (3 mmol, 636 mg) were added to the flask. The reaction was stirred at room temperature until the starting material disappeared on TLC. The solvent was evaporated, and the remaining crude was purified with C-18 reverse phase flash column to yield **40**. White solid (75% yield over 2 steps). MS (ESI): *m/z* calculated for C₃₄H₃₅N₂O₄ [M + H]⁺ 535.26, found 535.23. ¹H NMR (400 MHz, methanol-*d*₄) δ 7.80 (d, *J* = 7.6 Hz, 2H), 7.62 (dd, *J* = 15.7, 7.5 Hz, 2H), 7.48–7.35 (m, 12H), 7.33–7.25 (m, 2H), 4.43–4.05 (m, 7H), 3.25–3.03 (m, 2H), 2.55 (q, *J* = 8.3, 6.5 Hz, 1H), 2.46–2.20 (m, 1H), 1.35 (s, 3H). ¹³C NMR (101 MHz, MeOD) δ 176.68, 157.48, 145.26, 145.07, 142.58, 142.56, 132.20, 131.24, 130.45, 130.44, 128.86, 128.19, 126.29, 126.14, 120.98, 67.91, 58.81, 58.40, 48.28, 31.28, 24.16.

■ ASSOCIATED CONTENT

Supporting Information

The Supporting Information is available free of charge on the ACS Publications website at DOI: 10.1021/acs.jmedchem.6b01796.

Crystallography data collection and refinement statistics, inhibitory activity of compound **18** against SET1 family histone methyltransferases, stability test of compound **18** in cell culture, and experimental methods for HMT inhibition assay of compound **18** for other SET1 family members (PDF)

Binding model of WDR5 with compound **13** (PDB)

Molecular formula strings (CSV)

Accession Codes

The coordinates for the cocrystal structure for compounds **16** and **18** in complex with WDR5 have been deposited into PDB (PDB codes 4GMB and 5VFC).

■ AUTHOR INFORMATION

Corresponding Author

*Tel: 1-734-615-0362. Fax: 1-734-647-9647. E-mail: shaomeng@umich.edu.

ORCID

Shaomeng Wang: 0000-0002-8782-6950

Author Contributions

^ΔH.K., Y.L., L.L., J.J., and S.L. contributed equally.

Notes

The authors declare the following competing financial interest(s): Multiple patents have been filed by University of Michigan on these MLL-WDR5 inhibitors, which have been licensed by Ascentage Pharma Group. Shaomeng Wang, Hacer Karatas, Yali Dou, Yangbing Li, Liu Liu, and Denzil Bernard are inventors of these MLL-WDR5 inhibitors reported in this manuscript. Shaomeng Wang is a co-founder of Ascentage, owns stock in Ascentage, and serves as a consultant for Ascentage. The University of Michigan and Shaomeng Wang have also received a research contract from Ascentage.

■ ACKNOWLEDGMENTS

We are grateful for the financial support from the National Cancer Institute, National Institutes of Health (NIH) (Grant R01 CA177307 to S. Wang and Y. Dou), Leukemia and Lymphoma Society (to S. Wang), Leukemia and Lymphoma Society Scholar grant (to Y. Dou), and Ascentage Pharma Group (to S. Wang). Use of the Advanced Photon Source, an Office of Science User Facility operated for the U.S. Department of Energy (DOE) Office of Science by Argonne National Laboratory, was supported by the U.S. DOE under Contract No. DE-AC02-06CH11357. Use of the LS-CAT Sector 21 was supported by the Michigan Economic Development Corporation and the Michigan Technology Tri-Corridor (Grant 08SP1000817).

■ ABBREVIATIONS

WDR5, WD repeat domain 5 protein; MLL, mixed lineage leukemia; MLL1–4, mixed lineage leukemia 1–4; H3K4, histone 3 lysine 4; ALL, acute lymphoid leukemia; AML, acute myeloid leukemia; HMT, histone methyltransferase; Fmoc-OSu, 9-fluorenylmethyl *N*-succinimidyl carbonate; DIPEA, *N,N*-diisopropylethylamine; Pbf, 2,2,4,6,7-pentamethyldihydrobenzofuran-5-sulfonyl; EDCl, 1-ethyl-3-(3-(dimethylamino)propyl)carbodiimide; HOAt, 1-hydroxy-7-azabenzotriazole; DEA, diethylamine; HATU, 1-[bis(dimethylamino)methylene]-1*H*-1,2,3-triazolo[4,5-*b*]pyridinium 3-oxide hexafluorophosphate; DMF, dimethylformamide; TMS, tetramethylsilane; FP, fluorescence polarization

■ REFERENCES

- (1) Hess, J. L. MLL: A histone methyltransferase disrupted in leukemia. *Trends Mol. Med.* **2004**, *10*, 500–507.
- (2) Jude, C. D.; Climer, L.; Xu, D.; Artinger, E.; Fisher, J. K.; Ernst, P. Unique and independent roles for MLL in adult hematopoietic stem cells and progenitors. *Cell Stem Cell* **2007**, *1*, 324–337.
- (3) Meyer, C.; Hofmann, J.; Burmeister, T.; Gröger, D.; et al. The MLL recombinome of acute leukemias in 2013. *Leukemia* **2013**, *27*, 2165–2176.
- (4) Borkhardt, A.; Wuchter, C.; Viehmann, S.; Pils, S.; Teigler-Schlegel, A.; Stanulla, M.; Zimmermann, M.; Ludwig, W. D.; Janka-Schaub, G.; Schrappe, M.; Harbott, J. Infant acute lymphoblastic leukemia - combined cytogenetic, immunophenotypic and molecular analysis of 77 cases. *Leukemia* **2002**, *16*, 1685–1690.
- (5) Felix, C. A.; Lange, B. J.; Chessells, J. M. Pediatric Acute Lymphoblastic Leukemia: Challenges and Controversies in 2000. *Hematology Am. Soc. Hematol. Educ. Program* **2000**, *2000*, 285–302.
- (6) Krivtsov, A. V.; Armstrong, S. A. MLL translocations, histone modifications and leukaemia stem-cell development. *Nat. Rev. Cancer* **2007**, *7*, 823–833.
- (7) Thiel, A. T.; Blessington, P.; Zou, T.; Feather, D.; Wu, X.; Yan, J.; Zhang, H.; Liu, Z.; Ernst, P.; Koretzky, G. A.; Hua, X. MLL-AF9-induced leukemogenesis requires coexpression of the wild-type Mll allele. *Cancer Cell* **2010**, *17*, 148–159.
- (8) Milne, T. A.; Kim, J.; Wang, G. G.; Stadler, S. C.; Basrur, V.; Whitcomb, S. J.; Wang, Z.; Ruthenburg, A. J.; Elenitoba-Johnson, K. S.; Roeder, R. G.; Allis, C. D. Multiple interactions recruit MLL1 and MLL1 fusion proteins to the HOXA9 locus in leukemogenesis. *Mol. Cell* **2010**, *38*, 853–863.
- (9) Patel, A.; Vought, V. E.; Dharmarajan, V.; Cosgrove, M. S. A conserved arginine-containing motif crucial for the assembly and enzymatic activity of the mixed lineage leukemia protein-1 core complex. *J. Biol. Chem.* **2008**, *283*, 32162–32175.
- (10) Karatas, H.; Townsend, E. C.; Bernard, D.; Dou, Y.; Wang, S. Analysis of the binding of mixed lineage leukemia 1 (MLL1) and histone 3 peptides to WD repeat domain 5 (WDR5) for the design of

- inhibitors of the MLL1-WDR5 interaction. *J. Med. Chem.* **2010**, *53*, 5179–5185.
- (11) Karatas, H.; Townsend, E. C.; Cao, F.; Chen, Y.; Bernard, D.; Liu, L.; Lei, M.; Dou, Y.; Wang, S. High-affinity, small-molecule peptidomimetic inhibitors of MLL1/WDR5 protein-protein interaction. *J. Am. Chem. Soc.* **2013**, *135*, 669–682.
- (12) Dou, Y.; Milne, T. A.; Ruthenburg, A. J.; Lee, S.; Lee, J. W.; Verdine, G. L.; Allis, C. D.; Roeder, R. G. Regulation of MLL1 H3K4 methyltransferase activity by its core components. *Nat. Struct. Mol. Biol.* **2006**, *13*, 713–719.
- (13) Patel, A.; Dharmarajan, V.; Cosgrove, M. S. Structure of WDR5 bound to mixed lineage leukemia protein-1 peptide. *J. Biol. Chem.* **2008**, *283*, 32158–32161.
- (14) Cao, F.; Townsend, E. C.; Karatas, H.; Xu, J.; Li, L.; Lee, S.; Liu, L.; Chen, Y.; Ouillet, P.; Zhu, J.; Hess, J. L.; Atadja, P.; Lei, M.; Qin, Z. S.; Malek, S.; Wang, S.; Dou, Y. Targeting MLL1 H3K4 methyltransferase activity in mixed-lineage leukemia. *Mol. Cell* **2014**, *53*, 247–61.
- (15) Senisterra, G.; Wu, H.; Allali-Hassani, A.; Wasney, G. A.; Baryte-Lovejoy, D.; Dombrowski, L.; Dong, A.; Nguyen, K. T.; Smil, D.; Bolshan, Y.; Hajian, T.; He, H.; Seitova, A.; Chau, I.; Li, F.; Poda, G.; Couture, J. F.; Brown, P. J.; Al-Awar, R.; Schapira, M.; Arrowsmith, C. H.; Vedadi, M. Small-molecule inhibition of MLL activity by disruption of its interaction with WDR5. *Biochem. J.* **2013**, *449*, 151–159.
- (16) Getlik, M.; Smil, D.; Zepeda-Velazquez, C.; Bolshan, Y.; Poda, G.; Wu, H.; Dong, A.; Kuznetsova, E.; Marcellus, R.; Senisterra, G.; Dombrowski, L.; Hajian, T.; Kiyota, T.; Schapira, M.; Arrowsmith, C. H.; Brown, P. J.; Vedadi, M.; Al-Awar, R. Structure-based optimization of a small molecule antagonist of the interaction between WD repeat-containing protein 5 (WDR5) and mixed-lineage leukemia 1 (MLL1). *J. Med. Chem.* **2016**, *59*, 2478–96.
- (17) Li, D. D.; Chen, W. L.; Wang, Z. H.; Xie, Y. Y.; Xu, X. L.; Jiang, Z. Y.; Zhang, X. J.; You, Q. D.; Guo, X. K. High-affinity small molecular blockers of mixed lineage leukemia 1 (MLL1)-WDR5 interaction inhibit MLL1 complex H3K4 methyltransferase activity. *Eur. J. Med. Chem.* **2016**, *124*, 480–489.
- (18) Li, D. D.; Chen, W. L.; Xu, X. L.; Jiang, F.; Wang, L.; Xie, Y. Y.; Zhang, X. J.; Guo, X. K.; You, Q. D.; Sun, H. P. Structure-based design and synthesis of small molecular inhibitors disturbing the interaction of MLL1-WDR5. *Eur. J. Med. Chem.* **2016**, *118*, 1–8.
- (19) Li, D. D.; Wang, Z. H.; Chen, W. L.; Xie, Y. Y.; You, Q. D.; Guo, X. K. Structure-based design of ester compounds to inhibit MLL complex catalytic activity by targeting mixed lineage leukemia 1 (MLL1)-WDR5 interaction. *Bioorg. Med. Chem.* **2016**, *24*, 6109–6118.
- (20) Grebien, F.; Vedadi, M.; Getlik, M.; Giambro, R.; Grover, A.; Avellino, R.; Skucha, A.; Vittori, S.; Kuznetsova, E.; Smil, D.; Baryte-Lovejoy, D.; Li, F.; Poda, G.; Schapira, M.; Wu, H.; Dong, A.; Senisterra, G.; Stukalov, A.; Huber, K. V.; Schonegger, A.; Marcellus, R.; Bilban, M.; Bock, C.; Brown, P. J.; Zuber, J.; Bennett, K. L.; Al-Awar, R.; Delwel, R.; Nerlov, C.; Arrowsmith, C. H.; Superti-Furga, G. Pharmacological targeting of the Wdr5-MLL interaction in C/EBPalpha N-terminal leukemia. *Nat. Chem. Biol.* **2015**, *11*, 571–578.
- (21) Knutson, S. K.; Wigle, T. J.; Warholc, N. M.; Sneeringer, C. J.; Allain, C. J.; Klaus, C. R.; Sacks, J. D.; Raimondi, A.; Majer, C. R.; Song, J.; Scott, M. P.; Jin, L.; Smith, J. J.; Olhava, E. J.; Chesworth, R.; Moyer, M. P.; Richon, V. M.; Copeland, R. A.; Keilhack, H.; Pollock, R. M.; Kuntz, K. W. A selective inhibitor of EZH2 blocks H3K27 methylation and kills mutant lymphoma cells. *Nat. Chem. Biol.* **2012**, *8*, 890–896.
- (22) Daigle, S. R.; Olhava, E. J.; Therkelsen, C. A.; Majer, C. R.; Sneeringer, C. J.; Song, J.; Johnston, L. D.; Scott, M. P.; Smith, J. J.; Xiao, Y.; Jin, L.; Kuntz, K. W.; Chesworth, R.; Moyer, M. P.; Bernt, K. M.; Tseng, J. C.; Kung, A. L.; Armstrong, S. A.; Copeland, R. A.; Richon, V. M.; Pollock, R. M. Selective killing of mixed lineage leukemia cells by a potent small-molecule DOT1L inhibitor. *Cancer Cell* **2011**, *20*, 53–65.
- (23) Nielsen, P. R.; Nietlispach, D.; Mott, H. R.; Callaghan, J.; Bannister, A.; Kouzarides, T.; Murzin, A. G.; Murzina, N. V.; Laue, E. D. Structure of the HP1 chromodomain bound to histone H3 methylated at lysine 9. *Nature* **2002**, *416*, 103–107.
- (24) Otwinowski, Z.; Minor, W. Processing of x-ray diffraction data collected in oscillation mode. *Methods Enzymol.* **1997**, *276*, 307–326.
- (25) McCoy, A. J.; Grosse-Kunstleve, R. W.; Adams, P. D.; Winn, M. D.; Storoni, L. C.; Read, R. J. Phaser crystallographic software. *J. Appl. Crystallogr.* **2007**, *40*, 658–674.
- (26) Couture, J. F.; Collazo, E.; Trievel, R. C. Molecular recognition of histone H3 by the WD40 protein WDR5. *Nat. Struct. Mol. Biol.* **2006**, *13*, 698–703.
- (27) Adams, P. D.; Grosse-Kunstleve, R. W.; Hung, L. W.; Ioerger, T. R.; McCoy, A. J.; Moriarty, N. W.; Read, R. J.; Sacchettini, J. C.; Sauter, N. K.; Terwilliger, T. C. PHENIX: Building new software for automated crystallographic structure determination. *Acta Crystallogr., Sect. D: Biol. Crystallogr.* **2002**, *58*, 1948–1954.
- (28) Emsley, P.; Cowtan, K. Coot: Model-building tools for molecular graphics. *Acta Crystallogr., Sect. D: Biol. Crystallogr.* **2004**, *60*, 2126–2132.
- (29) Vagin, A.; Teplyakov, A. MOLREP: An automated program for molecular replacement. *J. Appl. Crystallogr.* **1997**, *30*, 1022–1025.
- (30) Bricogne, G.; Blanc, E.; Brandl, M.; Flensburg, C.; Keller, P.; Paciorek, W.; Roversi, P.; Sharff, A.; Smart, O. S.; Vonrhein, C.; Womack, T. O. BUSTER, 2.10.0., Global Phasing Ltd., Cambridge, United Kingdom, 2011.
- (31) Jones, G.; Willett, P.; Glen, R. C.; Leach, A. R.; Taylor, R. Development and validation of a genetic algorithm for flexible docking. *J. Mol. Biol.* **1997**, *267*, 727–748.
- (32) Verdonk, M. L.; Cole, J. C.; Hartshorn, M. J.; Murray, C. W.; Taylor, R. D. Improved protein - ligand docking using GOLD. *Proteins* **2003**, *52*, 609–623.